Intensification of Catalytic Conversion for Production of Fuel-additive

Thesis

Submitted By

Arpan Kar

Exam Roll No.: M4CHE23003

Class Roll No.: 002110302004

Reg. No.: 160016 of 2021-2022

Under the guidance of

Prof. Rajat Chakraborty

A Thesis submitted in the fulfilment of the requirement for the degree of

MASTERS IN CHEMICAL ENGINEERING

DEPARTMENT OF CHEMICAL ENGINEERING

Jadavpur University

Jadavpur, Kolkata-700032

JULY, 2023

Declaration of Originality and Compliance of Academic Ethics

I hereby declare that this thesis contains literature survey and original research work by the undersigned candidate, as part of his "Master of Chemical Engineering" studies. All information in this document have been obtained and presented in accordance with academic rules and ethical conduct. I also declare that, as required by these rules and conduct, I have fully cited and referenced all material and results that are not original to this work.

Name: **Arpan Kar**

Exam Roll No.: **M4CHE23003**

Thesis Title:

Intensification of Catalytic Conversion for Production of Fuel-additive

Arpan Kar 27/07/2023

Signature and date:

July 2023

Certification

This is to certify that Mr. Arpan Kar, final year Masters of Chemical Engineering (M.E) examination student of the Department of Chemical Engineering, Jadavpur University (Exam Roll No.: M4CHE23003; Reg. No.:160016 of 2021-2022 has completed the project titled: - **"Intensification of Catalytic Conversion for Production of Fuel-additive"**, *under the guidance of Prof. Rajat Chakraborty during his Masters Curriculum. This work has not been reported earlier anywhere and can be approved for submission in partial fulfillment of the coarse work.*

27.07.2023

Prof. Rajat Chakraborty

Head of Department and Professor,
Chemical Engineering Department,
Jadavpur University.

HEAD
CHEMICAL ENGINEERING DEPARTMENT
JADAVPUR UNIVERSITY
Kolkata-700 032

27.07.2023

Prof. Rajat Chakraborty

Project Supervisor and Professor,
Chemical Engineering Department,
Jadavpur University.

Professor
CHEMICAL ENGINEERING DEPARTMENT
JADAVPUR UNIVERSITY
Kolkata-700 032

28/07/23

Prof. Ardhendu Ghoshal

Dean of Faculty and Engineering Technology,
Jadavpur University.

DEAN
Faculty of Engineering & Technology
JADAVPUR UNIVERSITY
KOLKATA-700 032

Acknowledgement:

I wish to express my sincere gratitude to all the individuals who have contributed in various ways to the research and completion of this thesis. Their support and assistance have been invaluable and deserve special mention.

Firstly, I would like to acknowledge the guidance and supervision provided by Prof. Rajat Chakraborty, Head of Department and Project Supervisor. His expertise and encouragement throughout the research have been invaluable, and I am grateful for his unwavering support.

I am also grateful to the faculty members and staff of my department for their help and cooperation. The support of Jadavpur University, Dept. of Chemical Engineering, in providing access to equipment for my research is also greatly appreciated.

I extend my sincere thanks to my PhD senior, Mr. Sourav Barman, for his continuous support and guidance throughout the project period. My friends and colleagues have also provided valuable assistance, and I am grateful for their support.

I would like to express my deepest appreciation to my family for their unwavering support and encouragement throughout my master's degree programme.

Lastly, I acknowledge that it is not possible to list all those who have contributed to this thesis, but their views and tips have been invaluable and are greatly appreciated.

Table of Contents

Chapter 1

ABSTRACT

1.1 Abstract

A novel nano-photocatalyst has been prepared using hydroxyapatite (HAp) derived from waste fish scale and fly ash derived aluminosilicate (SiO2-Al2O3) grafted with zirconium oxide (ZrO2) active sites by innovative photo-hydrothermal protocol. The physio-chemical properties of the prepared photocatalyst have been characterized by different analyses like XRD, FTIR, XPS, UV-VIS-NIR, BET, NH3-TPD, HRTEM, DLS and TGA. The optimal catalyst has Zr loading of 20 wt% and has a low bandgap energy of 2.15 eV as confirmed by UV-VIS-NIR spectroscopy. The optimal catalyst also depicted a high acidity of 1.52 mmol NH3/g and a specific surface area of 62.872 m^2/g. Owing to the high acidity, specific surface area and low band gap energy the photocatalyst has led to achieve a yield of 76.6% levulinic acid (LA) from glucose in hybrid radiation reactor (HRR) deploying UV and FIR irradiation at appreciably low temperature and reaction time of 115°C and 2h respectively. Under the same reaction conditions, the conventionally heated reactor (CHR) gave a very low yield of 23.7 %. Individual radiation effects on LA yield evinced the synergistic advantageous effect of hybrid radiation technique. The catalyst reusability and regenerative study confirmed the high stability of the prepared catalyst. Also, a comparative LCI study has been conducted between HRR and CHR systems which revealed that HRR is more environmentally sustainable than CHR. HRR based process demonstrated a 59% lower global warming potential, 65% lower terrestrial ecotoxicity while being 120% more energy efficient than CHR based reaction making HRR more environmentally sustainable as well as economically feasible.

This study also focused on the synthesis of ethyl levulinate (EL) from glucose in ethanol medium, utilizing various catalytic systems. To replace conventional heating, a hybrid

radiation system combining UV and IR was implemented. The optimization of key reaction parameters, such as reaction temperature (140 ℃), reaction time (45 mins), catalyst loading (30 wt%), and glucose-to-ethanol molar ratio (90), was achieved using a Taguchi L9 orthogonal design. At the optimized conditions, the maximum EL yield of 76.08% with 100% selectivity was obtained using an Amberlyst-36 + TiO_2 (2:1) catalytic system. Furthermore, the synthesized EL was blended with biodiesel and commercial diesel at different ratios to evaluate engine performance and emission quality. The B7E3 blend exhibited favorable results, demonstrating a significant reduction of 19% and 18.86% in hydrocarbon (HC) and carbon monoxide (CO) emissions, respectively, compared to the other blends. Additionally, the B7E3 blend showcased lower brake specific fuel consumption (BSFC) and higher brake thermal efficiency (BTE). Furthermore, a life cycle assessment (LCA) was performed to evaluate the environmental impacts of EL production. in a conventional reactor (ELCH) in comparison to a hybrid radiation reactor (ELHR). The findings revealed that the ELHR significantly reduced global warming potential (GWP) by 48.86% compared to the ELCH, while also exhibiting a five-fold reduction in energy consumption. Overall, this study provides a comprehensive analysis of EL synthesis, engine performance, emission characteristics, and environmental implications, emphasizing the advantages of the hybrid radiation system over conventional heating methods.

1.2. Research highlights

- Production of platform chemical (levulinic acid) using a novel mixed support catalyst derived from waste fish scales and fly ash.
- Implementation of hybrid radiation to simulate natural sunlight.
- High LA yield of 63.71% from glucose has been achieved at a low temperature of 100°C and 2 h reaction time.
- HRR based reaction had a 59% lower global warming potential (GWP) than CHR based reaction.
- The HRR system is 120% more energy efficient than CHR.
- The cost of 1 kg ZFH2 catalyst is INR 806.58.
- Production of EL from glucose under hybrid radiation at yield as high as 76.08% with 100% selectivity.
- Study of different catalytic systems on EL yield.
- The effects of different radiation systems reveal the synergistic effects of UV and IR hybrid radiation which led to a rise in EL yield of 45-50% more than when individual radiations are used.
- Engine performance and emission study of diesel-biodiesel-EL blends which shows 18.86 % reduction in CO emission and 19 % reduction in HC emission.
- Reduction in GWP by 48.86 % in hybrid radiation (ELHR) reactor.
- ELHR is 5 times more efficient than conventionally heated (ELCH) reactor in terms of energy consumption.

Chapter 2

INTRODUCTION

2.1. Introduction

Energy is a crucial part of human society. Without energy the very social fabric to its entirety would collapse. We live in an era where we have mandated a continuous supply of electricity - energy in its useful form. A long power cut in a region would not only damage the economy but also cost people's lives. This is to prove how much dependent we are on energy supply. This reliance on energy is likely to exacerbate with technological innovation and population growth [1]. To mitigate the rising energy demand more supply of energy is necessary. Till now the global energy supply share is dominated by fossil fuels (> 80% of global energy supply) as depicted in Fig. 1 [2].

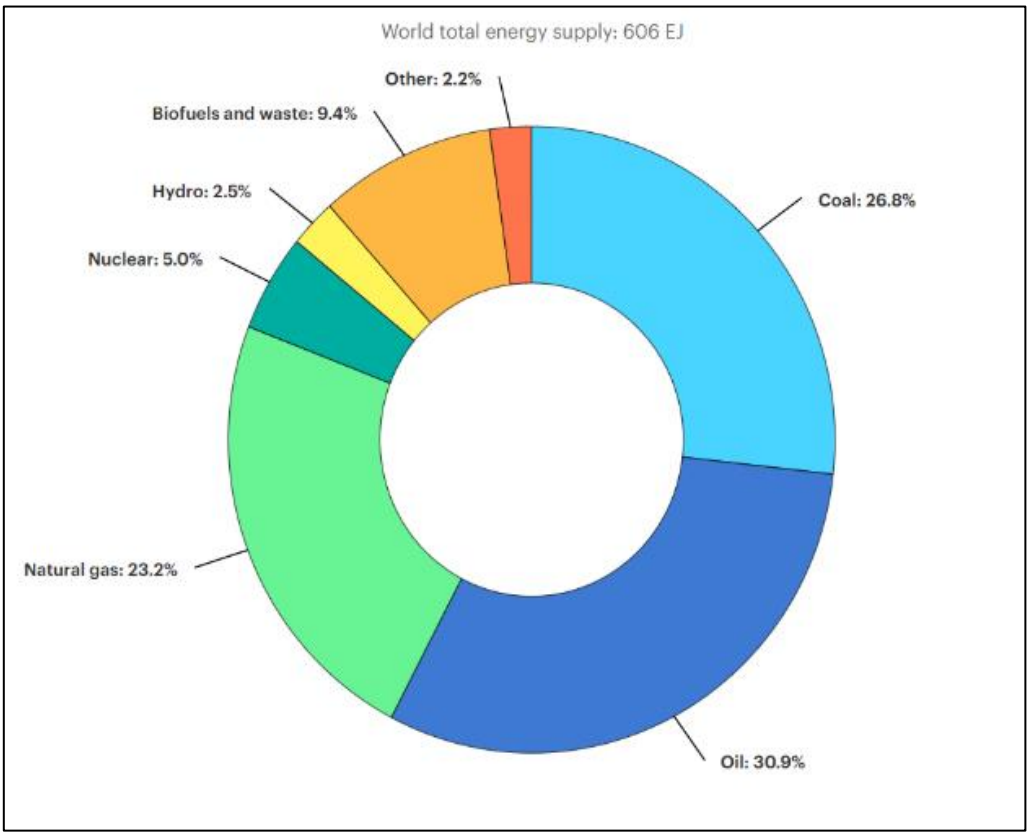

Figure 1. Global share of total energy supply by source.

With fossil fuel being the major source of energy supply, it imposes the question of sustainability of the future world. The main drawbacks that come with the use of

conventional source of energy is that fossil fuels are exhaustible source of energy and is a cause of various environmental concerns like global warming, air pollution, acid precipitation, rising sea level and destruction of ecosystem. So, in order to address the

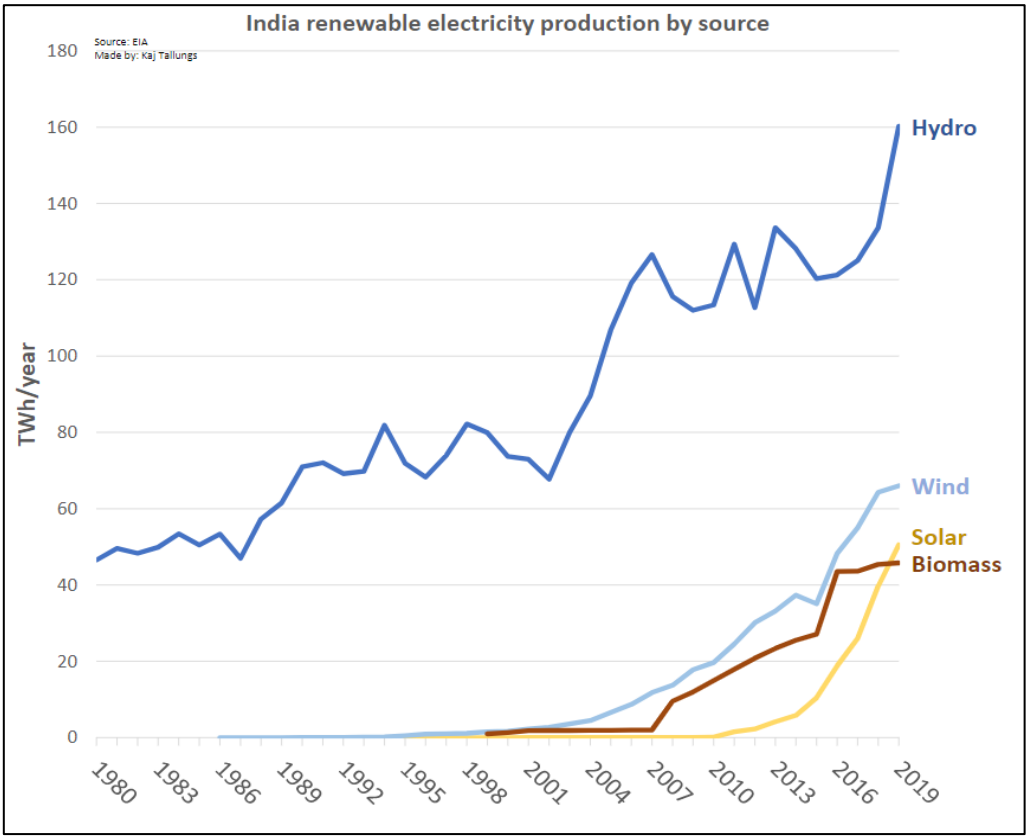

Figure 2. Renewable electricity production by source in India

adversities brought by consumption of fossil fuel it is high time to minimize its utilization and take refuge in a greener and sustainable source of energy. The main characteristics of such a source is that it has to be carbon neutral and renewable so that a cycle could be maintained.

The various sources of renewable energies in India are solar, wind, hydel power, biopower and nuclear power. India's rapidly growing economy, with a population of 1.3 billion, requires a significant amount of energy to meet its demands. Despite facing a power deficit at the time of independence, India has made progress towards energy

independence over the past seven decades. Today, India has an installed electricity capacity of over 400,000 MW, making it a power surplus nation. However, there are still challenges in ensuring reliable and affordable access to electricity for all citizens, particularly those in rural areas. To diversify its energy mix, India is increasing its reliance on renewable energy sources such as solar and wind power. India has been prioritizing the use of renewable energy in its power generation mix, in alignment with its sustainable development goals. With 40% of its installed electricity capacity coming from non-fossil fuel sources, India is the world's third-largest producer of renewable energy. The Indian government has set ambitious targets to increase the country's renewable energy capacity 500 GW by 2030. According to Ministry of New and Renewable Energy (MNRE), the shift towards renewable energy not only has environmental benefits but also economic advantages by reducing India's dependence on imported fossil fuels. According to a recent study sponsored by the MNRE, India has an estimated 750 million metric tonnes of biomass available annually. The study also found that there is a surplus biomass availability of about 230 million metric tonnes per year, which could potentially produce 28 GW of power using agricultural residues. In addition, sugar mills in India could generate an additional 14 GW of power through bagasse-based cogeneration if they adopt optimal levels of cogeneration to extract power from bagasse. The MNRE has recognized the potential of biomass energy and has implemented several programs to promote the use of efficient technologies for deriving maximum benefits across various sectors of the economy. Currently, most of India's biomass is being used to replace coal for steam generation, to produce biogas in rural areas or to produce biofuels. At present, India produces 1G biofuel (bioethanol & biodiesel) from agricultural feedstock. Much focus has been placed on production of 2G biofuel and various other value-added chemicals derived from waste biomass. In

this respect, levulinic acid is a key platform chemical that can be derived from glucose which again is derived through inedible lignocellulosic biomass valorization.

Levulinic acid has been identified as a promising building block for chemistry by the United States Department of Energy (DOE) in 2004 and 2010. The DOE has also included levulinic acid in its list of the Top 12 bio-based building blocks, which are used for synthesizing platform chemicals, liquid fuels, and fuel additives [3]. Fig. 3

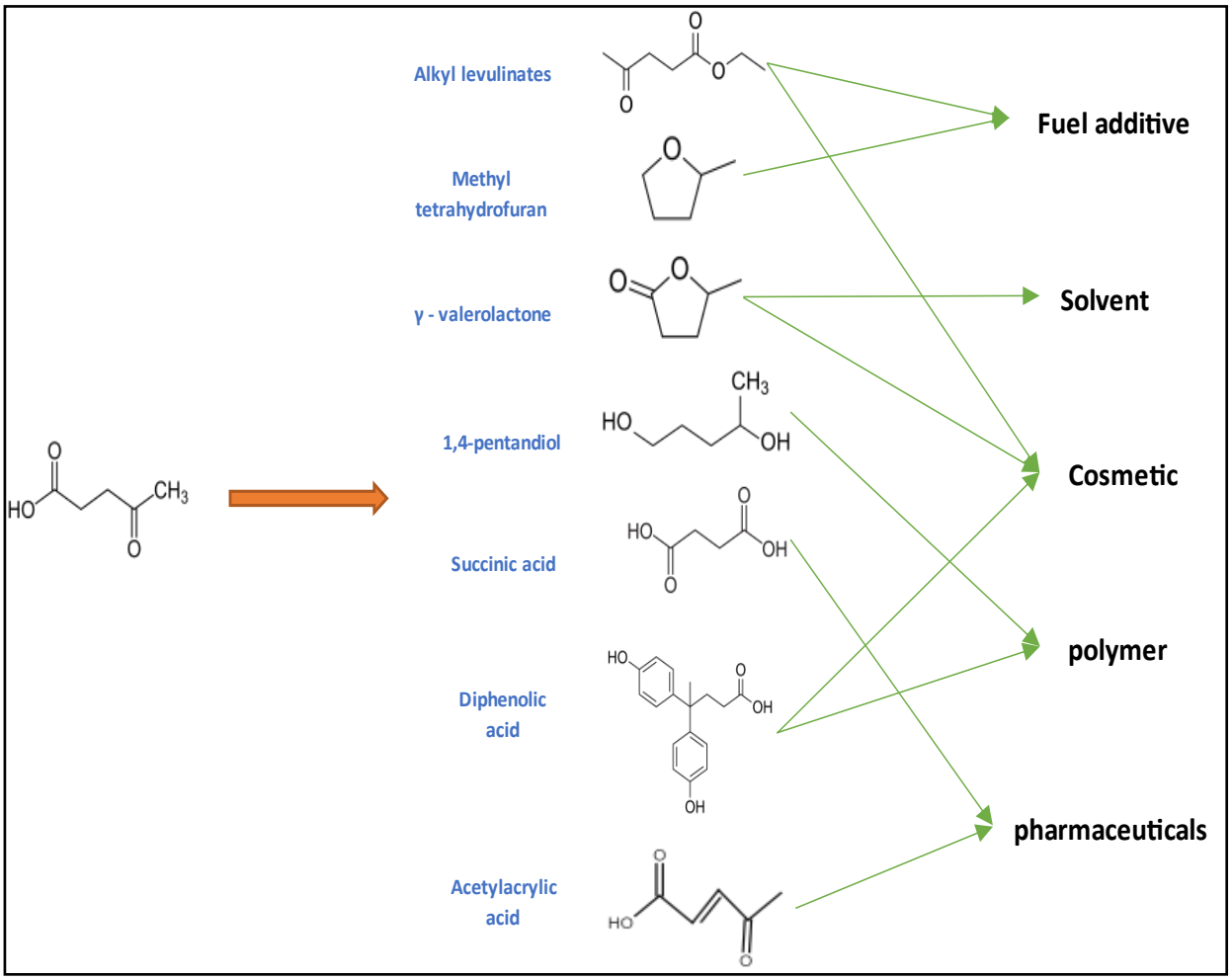

Figure 3. Various LA derivatives and their applications.

shows various products that can be synthesized from levulinic acid. Currently, LA is produced by acid catalyzed Biofine process from cellulosic source at high temperature. So, a milder sustainable LA production process is still a hot research topic owing to the versatility of LA as a platform chemical. LA can be synthesized mainly from C_6 sugars

derived by acid hydrolysis of lignocellulosic biomass. The hydrolysis proceeds via formation of 5-hydroxymethylfurfural (5-HMF) intermediate. Starting from glucose, the main reactions that occur are: (i) glucose isomerization into fructose; (ii) fructose dehydration into 5-HMF; and (iii) 5-HMF rehydration into LA. The schematic of this pathway is shown in Fig. 4. Although this synthetic route is the most thermodynamically favored pathway, there are some major drawbacks involved [4]. Firstly, the isomerization of glucose to fructose requires either a Bronsted base or a Lewis acid whereas, HMF dehydration is facilitated by the presence of Bronsted acid. An adjustment of Lewis-Bronsted acidity is required for optimal yield. Secondly, high temperature is required for conversion of glucose to LA. Such harsher reaction condition causes aldose degradation forming humin. To commercialize the production of LA, several important targets need to be achieved. Firstly, a selective dehydration process that minimizes the formation of humins/char is crucial to increase the yield of LA and reduce downstream processing costs. Secondly, using low-cost or negative-value biomasses as feedstocks is important to reduce the overall production cost of LA. This approach can also address sustainability concerns by reducing the use of food-based feedstocks. Thirdly, developing new, efficient catalysts to replace traditional inorganic mineral catalysts, such as H2SO4 and HCl, is essential to avoid equipment corrosion problems. These new catalysts should be selective, stable, and reusable. Lastly, removing impurities and other by-products from the hydrolysis liquor before recovering pure LA is important to obtain high-quality LA products. This can be achieved through effective separation and purification techniques. Overall, achieving these targets will enhance the commercial viability of LA production and promote its broader adoption across various industries.

Ethyl levulinate (EL), classified as a levulinate ester, has garnered recent attention as a prospective oxygenated additive for diesel fuel and a bio-based cold flow enhancer for biodiesel. [5]. Studies have indicated that a blend comprising 20% EL, 79% petroleum diesel, and 1% co-additive exhibited a notable oxygen content of 6.9%, surpassing the cleanliness of conventional diesel. This blend demonstrated favorable attributes such as enhanced lubricity, reduced sulfur content, and adherence to the stringent diesel fuel specifications outlined by ASTM D-975. Scientists have further investigated the distillation characteristics of EL-diesel blends and biodiesel blends incorporating fatty acid levulinate esters. Additionally, assessments encompassing pour points, cloud points and cold-filter-plugging points have been conducted on biodiesel blends derived from poultry fat and cottonseed oil, incorporating EL contents ranging from 2.5% to 20% by volume [6].

An extensive amount of research work has been conducted on EL synthesis over various catalytic system and feedstock [7,8]. Homogeneous catalysts like H2SO4 have been proven to give high EL yield but the use of such catalysts comes at the cost of low recyclability and high corrosivity [9]. So, the use of solid catalyst has been favored owing to their good recyclability, less corrosivity and high thermal stability. Zeolites have also been proven to be a reliable catalyst for EL synthesis with a yield of 40% [10]. A hybrid catalytic system of zeolite and mineral acid has also been adopted to raise the EL yield to 51.47% [11]. Resin catalysts with Bronsted acidity like Amberlyst-15 has shown high yield of 73% with fructose as feed [12]. Lewis acids like TiO_2 have also shown remarkable yield of 71% with fructose as feed [13]. It is interesting to observe that switch feed from fructose to glucose considerably reduce the EL yield. A novel process intensification technique utilizing radiation as heating source instead of conventional electrical has emerged. In this case, although microwave has been proven

to give high yields but it utilizes a lot of power [14]. But light intensification with UV/IR in presence of photocatalyst have shown remarkable outcome as depicted by Chakraborty et al. [15]. To the best of our knowledge EL synthesis has not been studied under the hybrid radiation method.

Most research on the utilization of diesel oxygenated additives has focused on biodiesel, and these studies have generally found that the addition of biodiesel has minimal or even positive effects on engine performance, reducing hydrocarbon (HC), carbon monoxide (CO), and particulate matter emissions, but often leading to higher nitrogen oxide (NOx) emissions [16]. In China, a study was conducted to investigate the performance and exhaust emissions of ethyl levulinate (EL) as an additive to diesel fuel. The study utilized a horizontal single-cylinder four-stroke diesel engine and examined various EL percentage blends [17]. The findings of these studies indicate that commercial diesel engines can effectively operate using EL-diesel blends containing up to 20% EL without requiring any modifications. Emission tests conducted under optimal engine operating conditions revealed certain trends. The HC emissions of EL-diesel blends, except for the 20% EL blend, were found to be higher than those of pure diesel fuel, albeit displaying a decreasing trend as the EL content increased. On the other hand, CO and NOx emissions exhibited an opposite pattern, with lower levels observed in low-level blends such as the 5% EL blend, but increasing as the EL content increased. Additionally, the smoke opacity of the EL-diesel blends consistently remained lower than that of pure diesel, with a decreasing trend observed as the EL content increased.

The examination of the synthesis and utilization of ethyl levulinate (EL) from carbohydrate resources has predominantly oriented towards technical facets. However, it is crucial to employ a life cycle assessment (LCA) to analyze the viability of EL

production from a sustainability perspective and its utilization in diesel engines. LCA serves as an evaluation tool that assesses the potential environmental impacts of a product or service throughout its entire life cycle. It is a universally embraced methodology. that enables the quantification of environmental impacts, identification of improvement opportunities, and determination of the most sustainable alternatives. As a result, LCA has gained significant recognition and widespread adoption as an integral part of environmental management practices. Very few studies related to EL production has conducted their LCA [18].

In this work, EL production from glucose has been studied in array of catalytic systems utilizing commercial catalysts under hybrid irradiation. Also, the effectiveness of EL as a potential diesel additive has been studied by blending with biodiesel and diesel through engine performance and emission quality. At the end an LCA study has been conducted to show the superiority of hybrid radiation method over conventional reactor in mitigating environmental impacts.

2.2. Role of catalysts in reaction

Catalysts play a vital role in chemical reactions by affecting the reaction kinetics. A positive catalyst is one that makes the reaction go faster by lowering its activation energy while a negative energy is one that slows down a reaction. A catalyst can be of two types depending upon its physical presence in a reaction mixture – homogeneous and heterogeneous. Homogeneous catalysts are the ones who have the same phase as that of the reactant while heterogeneous catalysts have distinct phase than the reactant. Homogeneous catalysts, such as mineral acids (HCl, H2SO4, HNO3, H3PO4) and soluble metal chlorides (FeCl3, AlCl3, ZnCl2, CuCl2), are commonly used in LA

production due to their low cost, easy availability, and high efficiency in producing high LA yields [19,20]. Their effectiveness depends on various factors, such as concentration, strength of primary dissociation constant, type and concentration of the feedstock, and reaction conditions. The use of homogeneous catalysts presents several disadvantages, such as difficulty in catalyst recovery for recycling, corrosion of equipment, and environmental pollution. The corrosive conditions also require special materials for reactor construction, increasing capital investment and operating costs. To address these issues, heterogeneous solid catalysts are being explored as a more cost-effective and environmentally friendly alternative. However, there is still a need for a simple and efficient process in LA biorefinery using cost-effective and environment-friendly catalysts.

Heterogenous catalyst generally comprise of a porous support material on which the active sites are doped. Supports play a crucial role in providing mechanical stability to catalyst nanoparticles or powders. They help to immobilize the particles, reducing their mobility and promoting chemical stabilization, and can be thought of as solid capping agents. In addition, supports enable the easy recycling of nanoparticles, reducing the overall cost of the catalyst. Therefore, choosing an appropriate support material is essential for ensuring the stability and activity of the catalyst, as well as for facilitating its recovery and reuse. Various types of catalyst support have used so far. The most popular catalyst support materials are activated carbon, metal oxides, CNTs etc. The precursors used in heterogeneous catalysts are generally expensive. So, in order to reduce cost of the catalyst the support material used are generally cheap. One sustainable and eco-friendly way to prepare a support is to utilize waste materials. Various waste materials used as catalyst support are fly ash, fish scales and animal bones derived hydroxyapatite, e-wastes like PCBs, activated carbon from waste

biomass. Utilization of these waste materials not only helps in reducing the cost of the catalyst but also helps in waste minimization.

Another very interesting catalyst type is photocatalyst. Semiconductor materials like TiO_2, ZnO, SnO_2, CuO, WO_3, ZnS, and CdS are the most common photocatalyst used [21,22]. In photocatalytic reactions, the process starts when light energy with an equal or greater value than the semiconductor's band gap stimulates an electron. This causes the transfer of the photoexcited electron from the valence band (VB) to the conduction band (CB), resulting in a hole in the CB. This hole acts as a potent oxidizing agent. The result of this process is the formation of electron-hole pairs (e-/h+), which can be created within femtoseconds (fs). The photoexcited charge carriers can then be trapped within shallow traps in picoseconds (ps) or deep traps in nanoseconds (ns). The hole

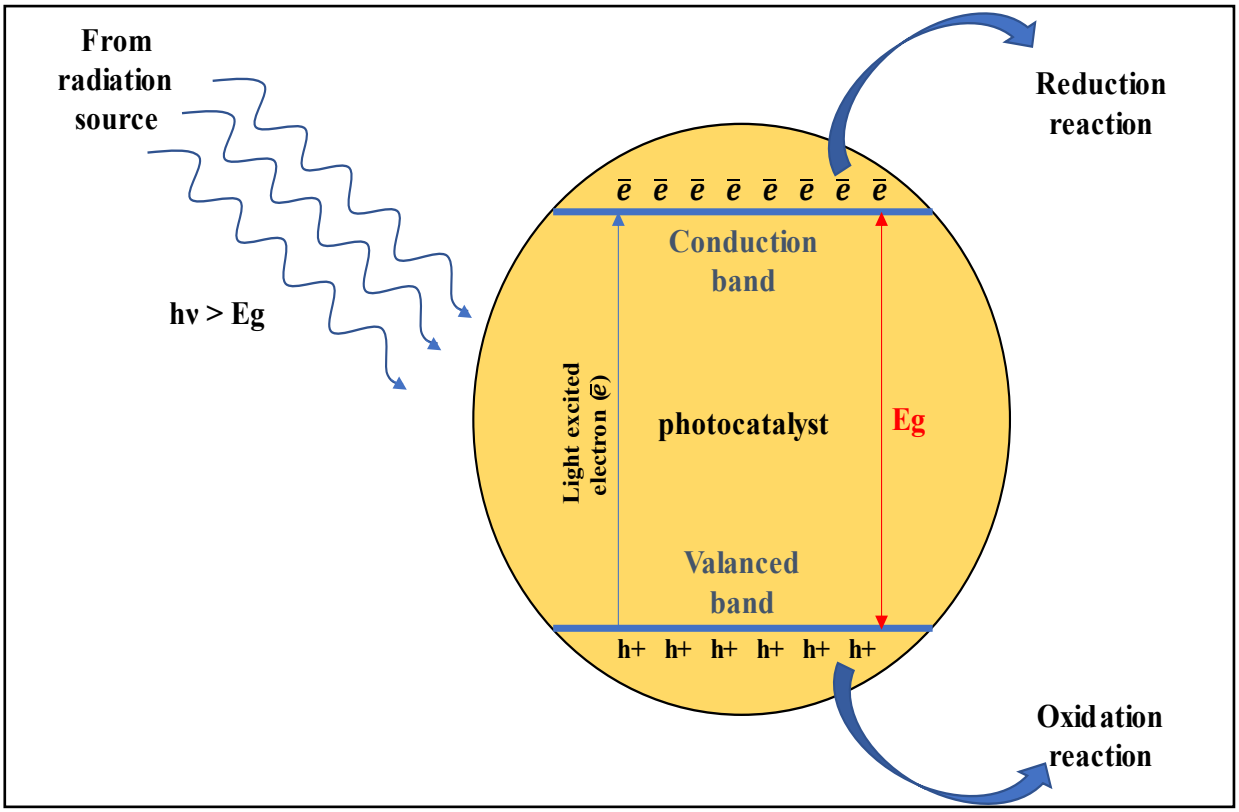

Figure 4. Photocatalytic process

and electron may recombine in a few tens of nanoseconds. Fig. 4 shows the photocatalytic mechanism.

Photocatalytic reactions using catalysts such as TiO_2 depend on the transfer of charges between the catalyst surface and organic compounds. This transfer can result in the direct oxidation or reduction of compounds or the generation of reactive oxidants such as hydroxyl radicals. In the case of TiO_2, UV light is commonly used as an energy source for photocatalytic oxidation due to its wide band gap [23]. The minimum band gap energy required for a photon to generate charge carriers over TiO_2 (anatase phase) is 3.2 eV, which corresponds to absorption of a 388 nm wavelength photon. As a result, TiO_2 photoactivation occurs in the UV region, specifically at wavelengths less than 388 nm. TiO_2 exists in three stable polymorphs, anatase (Eg = 3.2 eV), rutile (Eg = 3.02 eV), and brookite (Eg = 3.14 eV), with anatase being the most efficient form for conjugate reactions involving electrons. Combining the rutile and anatase phases has been suggested to increase TiO_2 photocatalytic activity, and the commercial catalyst Degussa P25 TiO_2, which contains 75% anatase and 25% rutile, is frequently used for this purpose [24].

The use of nano-catalysts enhances the transfer of electrons to the surface, allowing them to react with electron acceptors over a shorter distance compared to microstructures. Consequently, the recombination rate in nanostructures is lower. Several factors, including crystallite size, specific surface area, pore structure, pore volume, and crystalline phases, significantly impact the photocatalytic performance [25]. The high surface area and density of nano-sized catalysts improve their photoactivity and overall performance. It has been observed that certain transition elements when doped on photocatalysts like TiO_2, enhances the photocatalytic activity. This is due to the formation of metastable secondary conduction band which results in

increasing the lifetime of the photogenerated charge carriers. Also, the transition elements have vacant orbitals which make them very good Lewis acid. Levulinic acid production from various sources have been studied in presence of many transition metals.

Light intensification of a chemical reaction is a developing science. Non-ionizing radiations – not harmful to human – like microwave, infrared, visible and ultraviolet have been used for photo-thermal chemical process as a replacement of traditional heating. The main advantages of light intensification process are, 1) homogeneous heating, 2) less energy intensive (except for microwave) and 3) product selectivity sometimes increases because the reaction follows a totally different reaction pathway. Albeit, no photocatalytic reactor has been successfully implemented on an industrial scale.

In the present study, we have developed a cost-effective solid acid catalyst with waste fish scale derived hydroxyapatite and fly ash as support and ZrO2 active sites for glucose conversion to LA. To the best of our knowledge, no work involving a mixed support derived from waste materials have been published previously. The mixed support is expected to provide Bronsted acidity (HAp) as well a porous matrix (FA) for the catalyst. Hybrid radiation simulating natural sunlight has been implemented as a replacement for conventional heating which also activates the photocatalyst used in the reaction. Taguchi orthogonal design has been employed to optimize the LA production process. Moreover, the efficiency of HRR system compared to CHR system in terms of energy consumption has also been studied. Finally, the environmental impact assessment and sustainability of the overall process has been investigated through LCA methodology.

Chapter 3

LITERATURE REVIEW

3.1. Glucose to levulinic acid

3.1.1. Homogeneous catalysts system

- **Szabolcs et al.** [26] :- In this study, researchers found that saccharides can be converted to levulinic acid using microwave dielectric heating in the presence of sulfuric acid and hydrochloric acid. It was discovered that chlorine-containing catalysts could be avoided without compromising the yield of transformation significantly. The use of microwave irradiation as a heating method significantly reduced the reaction time compared to conventional heating, but did not affect the product yield. The optimal temperature for fructose and glucose decomposition was found to be 170°C, with a reaction time of 30 minutes, while cellulose had an optimal reaction time of 50 minutes. The corresponding LA yield from fructose, glucose and cellulose in presence of sulfuric acid were 27.5 wt%, 26.1 wt%, 15.4 wt% and that in presence of hydrochloric acid were 31.8 wt%, 31.4 wt%, 31.0 wt% respectively.

- **Zandvoort et al.** [27] :- The study analyzed the byproducts formed during the acid-catalyzed dehydration of sugars, specifically focusing on the furan-rich network formed via hydroxymethyl furfural. The molecular structure of humins was proposed based on multiple analytical techniques. The study utilized a DoE-based approach to investigate the influence of acid concentration, sugar intake, and temperature on humin formation from glucose. The results revealed that humin formation was strongly influenced by temperature and acid concentration, while sugar concentration had minimal statistical significance. Interestingly, the conditions that promoted high humin production were

opposite to those that favored high yields in LA. The HPLC analysis showed that C6 sugars mainly produced LA, while C5 sugars yielded furfural. The LA yields of 27 % and 31 % were obtained from glucose and fructose at temperature 180 ℃ and reaction time of 6 h in presence of 0.01 M sulfuric acid and 1 M sugar solution.

- **Rackemann et al.** [28] :- The study compared the effectiveness of methane sulfonic acid (MSA) and sulfuric acid in converting glucose and xylose mixtures into levulinic acid and furfural. It was found that high LA yields of 44.02 % could be achieved quickly by using a fast heating rate (180 ℃, 6 h). Furfural production was highest at lower feed concentrations due to enhanced degradation at higher concentrations. In the presence of xylose, there was a slight increase in levulinic acid yield, but this also led to a higher amount of solid residue. This residue matrix trapped small amounts of catalyst and products, and its aromatic, oligomeric, and carbonyl content increased with reaction temperature, time, and xylose concentration.

- **Choudhary et al.** [29] :- This study investigates the combined effect of Lewis ($CrCl_3$) and Brønsted (HCl) acid catalysis on the conversion of aldoses (glucose) to ketoses (fructose) to furans (HMF) to levulinic and formic acids. The results indicate that $CrCl_3$ is a highly effective catalyst for glucose isomerization to fructose in aqueous media. The hydrolysis of the Cr(III) ion releases H^+ ions, decreasing the solution pH. This intrinsic Brønsted acidity, derived from the Lewis acid, is primarily responsible for the dehydration of fructose to HMF and its subsequent hydrolysis to levulinic acid at low temperatures when no external Brønsted acids are added. It was also found that

the Lewis acid catalyst promotes side reactions, increasing the overall rate of disappearance of ketoses (fructose) and furans (HMF). While $CrCl_3$ can isomerize glucose to fructose and drive the Brønsted acid catalyzed dehydration/rehydration reactions, it is not selective in the HMF and levulinic acid production when used alone. Among the various Cr ions generated in aqueous media, $CrOH^{2+}$ is believed to be the most active for the aldose-to-ketose isomerization and may exhibit a Lewis acid−Brønsted base bifunctional behavior. The study also demonstrates that Brønsted acid catalysts inhibit the Lewis acid catalyzed isomerization by decreasing the concentration of the active Cr species $CrOH^{2+}$ due to a shift in the chemical equilibrium of metal cation hydrolysis. The interplay between the two acids indicates that optimizing the concentrations of Lewis and Brønsted acids in the cascade reactions to maximize the desired product yield is feasible and advisable. For instance, the study achieved high yields of glucose to levulinic acid in a single aqueous phase (46%) and to HMF in a biphasic system (59%) at a moderate reaction temperature (413 K) by combining $CrCl_3$ (Lewis acid) with HCl (Brønsted acid).

- **Peng et al.** [30] :- The study showed that different metal chlorides have varying effects on the conversion of cellulose, with some demonstrating higher catalytic activity than others. Specifically, transition metal chlorides such as $CrCl_3$, $FeCl_3$, and $CuCl_2$, as well as a group IIIA metal chloride ($AlCl_3$), displayed better catalytic activity for the reaction. Although the acidity of the reaction system due to the addition of metal chlorides was linked to the catalytic performance, the type of metal chloride used had a more significant impact. Various factors, such as reaction time, temperature, catalyst dosage, and

substrate concentration during cellulose degradation, played significant roles in the production of LA. The study identified the highest yield of LA to be 67 mol % when CrCl3 was used as the catalyst. Using CrCl3 as a catalyst requires less material and has the added advantage of being able to easily separate chromium metal from the reaction products and recycle it. Most of the chromium metal was present in its oxide form in the solid products, with only a small part in solution as Cr3+ ion. In summary, this study sheds light on the use of metal chlorides as catalysts for cellulose conversion and emphasizes the importance of selecting the appropriate type of metal chloride for optimal catalytic performance.

- **Shen et al.** [31] :- A highly efficient method for catalytic synthesis of 5-HMF and LA from monosaccharides has been developed using InCl3–H2O medium. A 79% yield of 5-HMF (in 15 minutes) and a 45% yield of LA (in 60 minutes) were achieved at 180 °C using only 2.5 mol% InCl3. The conversion rate of fructose was found to be higher than that of glucose, and the yield of 5-HMF was higher for fructose compared to glucose due to the stable ring structure of glucose. Fructose underwent both dehydration to 5-HMF and isomerization to glucose simultaneously in the InCl3–H2O medium. Notably, the dehydration process was preferred over isomerization in the presence of InCl3–H2O medium.

- **Fu et al.** [32] :- The synergistic catalytic activity of four organic Lewis acids, including samarium(III), aluminum(III), yttrium(III), and indium(III) trifluoromethanesulfonates, was examined with four organic Brønsted acids, including benzenesulfonic, toluene-p-sulfonic, trichloroacetic, and oxalic acids,

for the decomposition of glucose into levulinic acid (LA). The combination of aluminum trifluoromethane sulfonate (Al(CF3SO3)3) and oxalic acid (H2C2O4) was found to exhibit strong synergistic activity in decomposing glucose to LA. To investigate the effect of the mole fraction of Al(CF3SO3)3 in the Al(CF3SO3)3-H2C2O4 system on the decomposition of glucose, fructose, and 5-hydroxymethylfurfural (5-HMF), different concentrations were tested. The mixed-acid system demonstrated the strongest synergic catalytic activity for glucose, fructose, and 5-HMF decompositions at the Al(CF3SO3)3 mole fraction of 0.33. Additionally, the impact of temperature on the decomposition of glucose in the Al(CF3SO3)3-H2C2O4 system was examined. When glucose was subjected to decomposition with a H2C2O4 concentration of 0.015 mol/L at 180 °C for a period of 5 hours, the resulting yield and selectivity of levulinic acid (LA) were observed to be only 3.3% and 7.1%, respectively. In contrast, the use of pure Al(CF3SO3)3 resulted in a yield and selectivity of LA of 9.8%. However, the utilization of the Al(CF3SO3)3-H2C2O4 system led to a significant increase in the yield and selectivity of LA to 39.9%. These results highlight the substantial improvement in the efficiency of glucose decomposition achieved through the synergistic catalytic activity of organic Lewis and Brønsted acids.

3.1.2. Heterogeneous catalyst system

- **Zuo et al.** [33] :- This study involves the synthesis of a novel solid-acid catalyst based on CP resin, which was achieved by replacing some of the chlorine atoms with sulfonic groups. The researchers were able to control the amount of sulfonic groups on the catalyst, which acted as strong Brønsted acid sites that were stable in water due to covalent bonding to the catalyst support. The newly

synthesized CP-SO3H-1.69 catalyst exhibited promising results, converting glucose directly into LA with a 44.2% yield in an aqueous system. The same catalyst was able to convert microcrystalline cellulose into LA with a yield of 33% at an initial cellulose concentration of 4.8 wt%. By using 90 wt% GVL/10 wt% water as the reaction medium, a high yield of 65% was achieved. Although the catalyst was significantly deactivated after the reaction, its activity could be fully recovered by stirring the used catalyst in 28.5 wt% H2O2 at 35°C overnight. This study provides a new approach to preparing solid-acid catalysts, which not only focuses on anchoring sufficient acid sites to the catalyst support but also considers selecting an appropriate catalyst support to ensure easy access of cellulose to the catalytic site.

- **Son et al.** [34] :- This study focused on the production of levulinic acid from fructose under mild reaction conditions in water, using solid acid catalysts. The researchers conducted the reaction at various temperatures and with varying amounts of catalysts to identify the optimal reaction conditions. The study compared the performance of different heterogeneous catalysts and found that Amberlyst-15 produced the highest LA yield (52%) with the lowest HMF yield (below 3%) under the optimal conditions. To isolate levulinic acid from the reaction mixture, the researchers employed a rotary vacuum evaporator, resulting in a 47% isolated yield. Recycling experiments revealed that Amberlyst-15 maintained good activity after five runs, although the LA yield gradually decreased from 52% to 30%. The study also showed that the dehydration of fructose to LA using Amberlyst-15 outperformed other tested solid acid catalysts.

- **Zeng et al.** [35] :- In the present study, Al-Zr mixed oxides were synthesized using the coprecipitation method with different molar ratios, and their catalytic activities in glucose conversion under 180°C and 1.7 MPa hot compressed water were investigated. The prepared oxides exhibited solid solutions, and their acid-base properties were found to be influenced by their composition and structure. The amount of Zr in the mixed oxides affected the strength of both the strong acid and base sites, whereas moderate base sites were strengthened by Zr. The results of the activity test and catalyst characterization revealed that the formation of HMF or LA required different acid strengths. The yield of LA increased with an increase in the strength of the acid sites. The prepared oxides showed excellent catalytic activity, increasing glucose conversion from 46.6% to 85%. Furthermore, the formation of lactic acid required not only strong base sites but also moderate ones, especially those with suitable strength.

- **Ya'aini et al.** [36] :- This study focused on the preparation of hybrid catalysts using the wetness impregnation method. The catalysts were composed of CrCl3 and HY zeolite at weight ratios of 1:1, 1:2, and 2:1. Thermal gravimetric analysis indicated that there was interaction between CrCl3 and HY zeolite during the impregnation process. The catalytic performance of the hybrid catalysts was influenced by the type, amount, and strength of the acid sites, as well as surface area, hierarchy factor, and shape selectivity. Hybrid catalyst 1:2 displayed the highest hierarchy factor of 0.1637, followed by hybrid 1:1, hybrid 2:1, and HY zeolite catalysts. However, hybrid catalyst 1:1 had the highest number of reactive acid sites (13.13 μmol/m^2) on the catalyst surface, resulting

in the highest catalytic performance. This catalyst achieved a levulinic acid yield of 62% at 160 C for a reaction time of 180 minutes.

- **Ramli et al.** [37] :- The present study focused on the investigation of glucose decomposition over a Fe/HY zeolite catalyst in a batch reactor at temperatures ranging from 120 to 200 °C and reaction times of 0 to 240 minutes. The catalyst showed the highest LA yield of 66% at 100% glucose conversion at 180 °C. A kinetic model was developed to investigate the reaction kinetics of glucose conversion to LA, which involved four reactions with the main products being 5-HMF and LA, and humins as the insoluble by-product. External and internal diffusion effects were eliminated to use a pseudo-homogeneous reaction model for the kinetic modeling, and the kinetic was found to be first-order with a good agreement between the experimental and modeling data. The activation energies obtained from the model were lower compared to the values reported in previous literature, and the results of this study can be useful for process modeling applications.

- **Upare et al.** [38] :- In this study, GO-SO3H was identified as a highly effective catalyst for the selective synthesis of levulinic acid from glucose via a single-step hydrolysis process. The catalytic reaction achieved a maximum glucose conversion rate of 96.8% and a levulinic acid yield of 84% within 150 minutes, although the formation of char was also observed at a higher rate. The active sites responsible for the reaction are the Brønsted acid SO3H sites, but other functional groups such as carboxyl and hydroxyl are also crucial for enhancing glucose (and other biomass chemicals) adsorption. The layered morphology of GO-SO3H facilitates rapid diffusion of reactants and products, while the

sulfonate groups are thermally stable and do not leach into the reaction mixture. The catalyst can be recycled with only a minor decrease in activity and can be used as an initial bio-based cellulose feedstock or other biobased sugars. Future research will focus on strategies to minimize char formation.

- **Kumar et al.** [39] :- GaHPMo, which is the Ga salt of molybdophosphoric acid, has been identified as a promising catalyst for the transformation of biomass into levulinic acid. Through hydrothermal reactions conducted under optimal conditions (T= 150 °C; t = 10 h; and GaHPMo to glucose ratio of 1:5), a levulinic acid yield of 56 wt.% was obtained. This suggests that GaHPMo could serve as a potential alternative to traditional mineral acids used in levulinic acid production from biomass. Compared to the parent HPMo, GaHPMo displayed superior catalytic activity in terms of glucose conversion and selectivity for LA production. The sonochemical irradiation method was used to prepare GaHPMo, which resulted in the simultaneous formation of GaHPMo and entrapment of polyoxometallate in gallium micro/nanoparticles (Ga@HPMo).

- **Zeng et al.** [40] :- The research study implemented an innovative approach by utilizing a MFI-type ZRP zeolite as a catalyst for glucose dehydration in subcritical water conditions of 453 K and 1.7 MPa. Although the incorporation of ZRP zeolite had only a marginal impact on glucose conversion, it significantly altered the product composition. The effectiveness of glucose conversion was found to be directly associated with the acidic number of the zeolites. The formation of LA necessitates a strong acidity. The pore structure of zeolites also has a significant influence on the reaction. The presence of mesopores in the ZRP zeolites promotes parallel reactions, which leads to a

reduction in LA formation. The study achieved a maximum LA yield of 35.8%, which indicates promising potential for future application.

- **Wang et al.** [41] :- A magnetic solid acid catalyst was developed using the $S_2O_8^{2-}/ZrO_2$-TiO_2-Fe_3O_4 method through chemical coprecipitation. The catalyst's properties and structures were characterized using various techniques such as IR, XRD, BET, and VSM. The resulting catalyst exhibited a tetragonal structure, BET area of 27.3 m2/g, and a BET pore diameter of 1.74 nm. Using the developed catalyst for synthesizing levulinic acid from glucose, the results showed that a levulinic acid yield of 70.2% and a 90% catalyst recovery can be achieved under the conditions of 30 g/L glucose concentration, 200 ℃ reaction temperature, and a 2-hour reaction time. Therefore, the developed magnetic solid acid catalyst has the potential to be used for industrial-scale production of levulinic acid, which is a valuable platform chemical for the manufacturing of various chemicals and materials.

- **Joshi et al.** [42] :- This study highlights the efficacy of zirconia under hydrothermal conditions for the hydrolysis of cellulose and its subsequent conversion to levulinic acid (LA) in a single step. The findings reveal that, under optimal reaction conditions, complete conversion of cellulose to LA with a yield of 53.9 mol% can be achieved, which is the best result reported in the literature thus far. The yield of LA is significantly influenced by various reaction parameters, including temperature, time, substrate concentration, and catalyst quantity. The zirconia catalyst can be recovered from the reaction mixture and reused multiple times without any loss of catalytic activity following calcination. The hydroxy form of zirconia exhibits similar Lewis acidity to other

reported solid acid catalysts, enabling the hydrolysis and dehydration reactions of cellulose under hydrothermal conditions. The study proposes a plausible mechanism for the hydrolysis of cellulose to LA in water catalyzed by zirconium hydroxide. In conclusion, this research suggests that hydrous zirconia, an environmentally-friendly catalyst with superior activity and abundant Lewis acidity, can be employed in various chemical transformations where acidity plays a crucial role.

- **Ding et al.** [43] :- A good yield of 52.9% of LA was achieved using Al-doped mesoporous niobium phosphate in an aqueous solution, surpassing the yields of any other solid acid catalysts reported to date. The high selectivity and yield of LA were attributed to the catalyst's strong acid strength and a suitable Brønsted/Lewis acid molar ratio (1.2:1). The addition of aluminum to niobium phosphate enhanced the strong Lewis and Brønsted acids, especially the strong Lewis acid, resulting in increased LA yield from cellulose, glucose, and HMF. The addition of (TfO)3La into the catalytic system containing another catalyst (HCl, (TfO)3H, niobium phosphate) further confirmed that a suitable ratio of Brønsted/Lewis acid is crucial for higher LA selectivity from HMF, as well as from cellulose. The developed catalyst has promising applications in the production of LA and its downstream chemicals. After the production of LA in an aqueous solution of cellulose, it can be completely converted to γ-valerolactone through hydrogenation over the Ru/C catalyst without further separation, making the process more efficient and sustainable. The successful implementation of this catalyst in the production of LA represents a significant contribution to the field of renewable energy and sustainable chemistry.

- **Liu et al.** [44] :- The aim of this study was to develop a Nb-containing catalytic system for the conversion of glucose to lactic acid. The Fe-NbP catalyst was found to have a high catalytic activity, resulting in a yield of 64.2% for glucose conversion to lactic acid in aqueous medium at 180°C in 3.0 hours. This excellent catalytic activity was attributed to the high total acid density, appropriate B/L acid ratio, and stable catalyst structure. The researchers also investigated the effects of various reaction parameters such as temperature, time, catalyst dosage, and substrate concentration on lactic acid production. Furthermore, the catalyst was found to be recyclable for up to four cycles without significant loss of activity. In summary, this study highlights the potential of Nb-containing catalysts for the conversion of glucose to lactic acid, with Fe-NbP showing promise due to its high catalytic activity and recyclability.

- **Abdouli et al.** [45] :- This study investigated the effect of UV irradiation on the catalytic conversion of glucose to value-added molecules using titanium dioxide at high temperatures (120-150 °C) in anaerobic conditions. The reaction was carried out in a batch reactor designed to combine high temperature/pressure and irradiation. The results showed that UV irradiation inhibited the catalytic performance of titanium dioxide for producing gluconic acid, but facilitated the selective formation of levulinic acid in high yield (approximately 60% at 150 °C), along with the co-production of ethylene and hydrogen in the gas phase. The formation of levulinic acid was attributed to the creation of Brønsted acidity in the reaction medium upon irradiation, as the titanium dioxide catalysts used in the study did not have intrinsic Brønsted acid sites in the reaction conditions. It was suggested that either the electronic changes of the TiO_2 under UV or the

formation of weak carboxylic acids could be responsible for the formation of levulinic acid. However, further investigations such as theoretical studies or in-situ demonstrations of water protolysis are necessary to confirm these hypotheses.

- **Qu et al.** [46] :- In this study, a solid acid catalyst consisting of SO_4^{2-}/ZrO_2 with weak, strong, and super strong acid sites was developed for the conversion of glucose into HMF and LA. Sulfuric acid was used to increase the total acid content of ZrO_2 and generate super strong acid sites. By adjusting the SO_4^{2-} load, the total acid amount and distribution of the catalyst could be controlled. The results of glucose conversion indicated that increasing the total acid content was beneficial for complete glucose conversion, but excessive strong acidity could lead to side reactions and the formation of humins. The weak acid sites helped to isomerize glucose into fructose, while the combined effect of strong acid and high temperature directly dehydrated glucose to produce HMF and LA without isomerization. The use of a biphasic solvent system improved the selectivity of HMF, and NaCl was found to play a key role in the stratification of water and THF. After optimizing the reaction conditions, the highest yield of HMF (61.84%) and LA (29.68%) was obtained at 160 °C. The system exhibited high catalytic performance, and the catalyst could be reused without significant loss in activity, making it economically and practically promising for large-scale applications. The successful coproduction of HMF and LA resulted in a higher yield of platform chemicals.

- **Jow et al.** [47] :- In this study, solid-acid LZY zeolite powder was used as a catalyst for the catalytic dehydration of molten D-fructose to HMF and levulinic

acid in a sealed batch reactor at 140°C. The product distribution was analyzed using HPLC after different reaction times (0 to 15 h), and it was found that the model for heterogeneous dehydration of o-fructose over the LZY zeolite catalyst was similar to the model for the homogeneous hydronium ion-catalyzed D-fructose dehydration. The maximum yield of levulinic acid was 0.432 g per 1.00 g of the original D-fructose after 15 h, while the net yield of HMF was only 0.044 g per 1.00 g of the original D-fructose. This high yield of levulinic acid was due to the strong dehydration ability of the Lewis acid sites present on the alumina-silica support of the LZY zeolite. On the other hand, the high selectivity was attributed to the molecular sieving capability of the LZY zeolite matrix, which confined the HMF molecule with a diameter of 0.82 nm within a 'cage' adjacent to the 0.75 nm pores of the LZY zeolite.

- **Chen et al.** [48] :- In this research, a solid superacid catalyst ($S_2O_8^{2-}$/ZrO_2–SiO_2–Sm_2O_3) was used to decompose steam-exploded rice straw (SERS) and produce levulinic acid (LA), a versatile platform chemical. The study demonstrated that the solid superacid catalyst could be a substitute for homogeneous acid in catalyzing LA production from SERS, and the addition of the solid superacid increased the LA yield. The research also revealed that the combination of steam explosion and superfine grinding of rice straw could enhance the accessibility of cellulose and reduce the particle size of rice straw, resulting in an increased LA yield. The optimal conditions for the production of LA were found to be 200°C, 10 min, 13.3% solid superacid to pretreated rice straw, and 1:15 solid-liquid ratio. Under these conditions, the LA yield of superfine grinding SERS was 70% of the theoretical yield, which was comparable to the homogeneous acid-catalyzed production of LA.

- **Shen et al.** [49] :- A novel method was developed for the conversion of cellulose and other carbohydrates to levulinic acid using eco-friendly, cellulase-mimetic solid acids in pure water. The solid acid catalyst, SO3H functionalized sucralose (SA), exhibited favorable catalytic activity due to its functional groups and mesoporous structure. With SA-SO3H, levulinic acid was produced from untreated cellulose with yields up to 51.5%. Furthermore, ball-milling pretreatment of cellulose enhanced the performance of the solid acid catalyst. The prepared catalyst could be regenerated using H2O2 and reused. Biomimetic catalysts have significant potential in the development of efficient transformation routes for lignocellulosic biomass into valuable chemicals. Using glucose as the starting material, yields of 61.5% levulinic acid were obtained under the same reaction conditions using the same cellulase-mimetic solid acid catalyst.

- **Liu et al.** [50] :- In this work, it has been discovered that SO2 present in hot water can act as a highly efficient catalyst for the conversion of cellulose into glucose, and subsequently into levulinic acid and other products. The presence of both molecular SO2 and H+ ions, generated through the ionization of H2SO3, work in tandem as catalysts, resulting in exceptional product yields and minimal reactor corrosion, especially when compared to the use of dilute sulfuric acid. The reaction temperature, duration, and amount of SO2 added are significant factors that influence the conversion of cellulose and the resulting product distribution. Notably, a glucose yield of 48.0% and a levulinic acid yield of 45.0% were achieved under optimal conditions. Furthermore, the SO2 present in the reaction mixture can be fully recovered through steam stripping, thus

providing an environmentally friendly process for converting cellulose into valuable chemicals.

- **Pyo et al.** [51] :- The present study investigated the heterogeneous catalytic dehydration of fructose and glucose using a strong cation exchange resin (hydrogen form) as an acid catalyst in an aqueous medium to produce levulinic acid (LA). The impact of various salts, such as NaCl, KCl, CaCl2, Na2CO3, and Na2SO4, on sugar conversion and LA yield was examined. The optimized reaction conditions resulted in a 74.6% yield of LA from 10% (w/w) fructose in a 10% (w/w) NaCl aqueous solution over 24 hours at 110 °C using the catalyst at 30% (w/w sugar). Similarly, 10% (w/w) glucose monohydrate was dehydrated directly to LA (with 70.7% yield) under comparable conditions but at 145 °C. The study showed that salts improved the rate of catalytic dehydration in the following order: Cl−>CO32− >SO42−. Consequently, a sustainable process for bio-based LA production could be achieved by combining high sugar concentration and heterogeneous catalysis in an aqueous system under relatively mild conditions.

3.2. Glucose to ethyl levulinate

- **Li et al. [52] :-** This study demonstrates the efficient conversion of biomass-derived carbohydrates, such as glucose, sucrose, and inulin, into the biofuel EMF (5-ethoxymethylfurfural), along with the byproduct EL (levulinic acid ethyl ester) using solid catalysts. The combination of H-USY (6) and Amberlyst-15 achieves high yields of EMF (40-60%) and 3-13% of EL in a one-pot, two-step reaction process. On the other hand, dealuminated beta zeolites, specifically DeAl-H-beta (12.5)-700 and DeAl-H-beta (19)-700, can provide similar yields of EMF (~40%) but through a single-step process. Furthermore, a promising yield of EMF (67%) and EL (4%), totaling 71%, is obtained from fructose using a combined catalytic system. The proposed reaction pathway involves fructose and EDFF (5-ethoxymethyl-2-furfural) as important intermediates derived from glucose, contributing to enhanced EMF yields with zeolite-based catalytic systems. Importantly, the dealuminated beta zeolites exhibit structural integrity in ethanol, enabling their reuse for at least five consecutive reaction cycles, making them sustainable catalysts for biomass conversion.
- **Xu et al. [53] :-** This study highlights the significant impact of reaction conditions on the yield of EL (levulinic acid ethyl ester) obtained from glucose in ethanol media. Lower CG0 (initial glucose concentration) proves favorable for enhancing the EL yield. While higher temperatures can accelerate the chemical reaction rate, they may also lead to unwanted side reactions, and increased acid catalyst concentrations might result in reduced EL yield. Additionally, the presence of water in the system leads to a substantial decrease in the EL yield. The kinetic analysis demonstrates that USY (a type of solid

catalyst) is more efficient than sulfuric acid in converting glucose to 5-ethoxymethyl-2-furaldehyde (EDFF, an intermediate in EMF production). Furthermore, the use of USY offers advantages for industrial applications, including the limitation of diethyl ether production and catalyst reusability.

- **Chang et al. [54] :-** The combination of extremely low acid concentration and USY catalyst proves to be an effective approach for one-pot production of EL (levulinic acid ethyl ester) from biomass. By employing a mixed acid catalytic system comprising 0.1% sulfuric acid and 2.0% USY, a higher EL yield of 51.47% from glucose can be achieved at 180°C and 120 minutes reaction time. Remarkably, the USY catalyst can be recovered and reused more than three times without significant deactivation. Furthermore, FRs (likely referring to furfural derivatives) serve as promising raw materials for the one-pot production of EL using this mixed acid catalytic system. Under the optimized conditions, an EL yield of 18.68% was attained, corresponding to a theoretical yield of 51.22%.
- **Li et al. [55] :-** The study explores the use of acid-base bifunctionalized FeZrOx nanocatalysts with superparamagnetism for the conversion of EL (levulinic acid ethyl ester) to GVL (gamma-valerolactone) using ethanol as both the hydrogen donor and solvent. Among the nanoparticles studied, ZrFeO(1:3)-300 demonstrated excellent performance, possessing well-distributed acid-base sites, moderate surface area, and pore size. This catalyst exhibited superior activity for EL conversion, achieving a high GVL yield of 87.2% at 230°C within 3 hours. A crucial advantage was the easy recovery of the nanocatalyst from reaction mixtures using an external magnetic force, allowing its reuse for at least four cycles with nearly constant activity, experiencing only a slight

decrease in GVL yield from 87.2% to 83.6%. Additionally, when combining ZrFeO(1:3)-300 with a solid acid HY2.6, they promoted the direct conversion of sugar to GVL, resulting in a moderate yield of up to 44.7%. These findings demonstrate the potential of these nanocatalysts for efficient and recyclable processes in biomass conversion to valuable chemicals.

- **Peng et al. [56] :-** The current investigation explores a catalytic process for converting glucose to ethyl levulinate using solid acid catalysts such as SZ (sulfated zirconia). Glucose is nearly completely consumed, and under optimal experimental conditions, the yield of ethyl levulinate reaches above 30 mol%. The SZ catalyst is recoverable from the resulting product mixture and can be reused multiple times after calcination, with no substantial change in the ethyl levulinate yield. The major liquid products are easily separated through fractionation, and excess ethanol is recycled. While solid acid catalysts may yield lower product outputs, they offer unparalleled advantages over traditional homogeneous acids, including recyclability and reduced equipment corrosion. Consequently, future studies will continue to focus on developing new and environmentally benign catalysts with higher activity for the formation of levulinate esters.

Chapter 4

AIMS & OBJECTIVES

4.1. Aims and Objectives for glucose conversion to levulinic acid

1. Production of levulinic acid – platform chemical – from glucose.

2. An inexpensive novel waste-derived mixed catalyst support would be developed for the photocatalyst.

3. The synergistic effect of hybrid radiation using UV-FIR radiators on product yield would be investigated. The possibility for replacing conventional heating by radiation has to verified as well.

4. The efficacy of hybrid radiation reactor (HRR) system over conventionally heated reactor (CHR) system in terms of energy consumption would be studied.

5. The cost analysis of the overall process would be carried out to study the economic viability of the overall production process.

6. The environmental impact assessment and sustainability of the overall process would be investigated through LCA methodology using OpenLCA software.

4.2. Aims and Objectives for glucose conversion to ethyl levulinate

1. Production of ethyl levulinate from glucose.

2. The synergistic effect of hybrid radiation using UV-FIR radiators on product yield would be investigated. The possibility for replacing conventional heating by radiation has to verified as well.

3. The efficacy of hybrid radiation reactor system over conventionally heated reactor system in terms of energy consumption would be studied.

4. Engine performance and emission study of fuels prepared by blending EL with commercial biodiesel and diesel fuels.

5. The environmental impact assessment and sustainability of the overall process would be investigated through LCA methodology using OpenLCA software

Chapter 5

MATERIALS

5.1. Materials required for production of LA from glucose

- ✓ Raw fly ash procured from Kolaghat Thermal Power Station.
- ✓ Waste fish scales collected from Jadavpur (INDIA) Supermarket.
- ✓ Deionized water (DI) from Abhishek Chemicals Ltd. and tap water
- ✓ D (+) – Glucose from Himedia Laboratories Pvt. Ltd.
- ✓ Zirconyl nitrate hydrate from Himedia Laboratories Pvt. Ltd.
- ✓ Ethanol from Tedia High Purity Solvents
- ✓ Sodium hydroxide pellets
- ✓ Ammonia solution (99%)
- ✓ Hydrochloric acid (98%)
- ✓ Acetonitrile

5.2. Materials required for production of EL from glucose

- ✓ D (+) – Glucose from Himedia Laboratories Pvt. Ltd.
- ✓ Ethanol from Tedia High Purity Solvents
- ✓ Amberlyst variants from Sigma Aldrich
- ✓ Diesel from local gas station
- ✓ Biodiesel from Emami Biotech
- ✓ Deionized water (DI) from Abhishek Chemicals Ltd. and tap water
- ✓ Acetonitrile

Chapter 6

METHODS

6.1. Methods for production of LA from glucose

6.1.1. Design of Experiment

To study the simultaneous effects of multiple experimental parameters as well as to determine the optimal operating condition the experimental design has been built in accordance with the Taguchi orthogonal design. The L9 orthogonal array (Table 2) developed in MINITAB-19 software with four independent factors and three levels (Table 1) namely, reaction temperature (Xtp), reaction time (Xtm), precursor loading (Xp) and glucose amount (Xg) are considered. The purpose of using Taguchi DOE is that the analysis can be executed within 9 experiments only instead of performing 81 experiments with good accuracy [57].

To determine the optimal values of the operating parameters corresponding to the maximum value of the response variable the signal to noise ratios (SN) were evaluated according to Eq. 1 and the criteria “larger the better” has been taken into consideration.

$$\frac{S}{N} = -10\log\left(\frac{1}{n}\sum_{k=1}^{n}\frac{1}{Y_k{}^2}\right) \qquad (1)$$

where, In the given context, 'k' represents the number of replicates, and 'n' denotes the number of trial experiments conducted with various parametric combinations as per Table 2 and Y is the response variable.

Table 1: Experimental factors and levels for levulinic acid production employing the developed ZFH catalyst.

Factors	Temperature (℃) X_{tp}	Time (min) X_{tm}	Precursor loading (wt%) X_p	Glucose amount (mmol) X_g
Level 1	70	90	10	1
Level 2	80	120	20	3
Level 3	90	150	30	5

Table 2: L9 orthogonal array experimental matrix at different operating conditions and corresponding mean LA yield (Y) and signal-to-noise (SN) ratio.						
Runs	X_{tp}	X_{tm}	X_p	X_g	Yield%	SN
1	80	90	10	1	27.033	28.6379
2	80	120	20	3	33.230	30.4306
3	80	150	30	5	28.966	29.2378
4	90	90	20	5	44.433	32.9541
5	90	120	30	1	43.000	32.6694
6	90	150	10	3	41.000	32.2557
7	100	90	30	3	55.633	34.9066
8	100	120	10	5	54.530	34.7327
9	100	150	20	1	63.710	36.0842

6.1.2. Catalyst Preparation

Raw fish scales were boiled in distilled water repeatedly to remove the flesh and slime layer attached to it. After drying in hot air oven at 70 °C, the scales were ground to form fine power and passed through 240 mesh. Raw fly ash was calcined at 900 °C to remove any carbonaceous matter. Calcined fly ash was then magnetically stirred to remove any iron particles. Then it was alkali treated using sodium hydroxide, filtered and dried. To prepare a catalyst with 10 wt% zirconium loading, 1 g of zirconyl nitrate was mixed with 9 g of support materials (SiO2-Al2O3 and HAp) in 2:1 wt ratio in 50 ml of DI water. The mixture was taken in three-necked flask and vigorously stirred in presence of infrared irradiation at 80 °C under total reflux for 3h. After this ammonium hydroxide solution was added dropwise for precipitation purpose at pH 10 and the mixture was left to age for 24h. After that the solution mixture was neutralized to pH 8 using 1M HCl, dried at 90 °C and calcined at 250 °C for 3h to prepare the ZFH1 catalyst. In a similar way, catalysts with 20 and 30 wt% precursor loadings were prepared and are named as ZFH2 and ZFH3 respectively.

6.1.3. Reactor setup and photocatalytic synthesis of levulinic acid

The conversion of glucose to levulinic acid was conducted in a one-pot reaction using UV-FIR hybrid radiation conditions. The reactions were carried out in a 250 ml conical flask with specified amount of glucose in 20 ml water and 20 wt% catalyst concentration. The reactor was placed inside a square insulated vessel with one UV radiator (power: 200 W, wavelength: 280nm-320 nm) and one FIR radiator (power: 250 W, wavelength: 3μm-1mm) mounted in its walls on the opposite ends. At the bottom of the vessel a magnetic stirrer was present on which the reactor assembly was installed. The reaction was conducted under simultaneous exposure of both the lights. The steady temperature could be achieved by varying the intensity of the lights by a regulator. The reaction temperature was controlled by a PID controller. Following the completion of each run within the specified time, the reaction mixture was cooled to room temperature and then filtered. The product was then analyzed by HPLC (Perkin Elmer 200 Series) using UV detector and water-acetonitrile mixture (60:40 v/v) as mobile phase with 1 ml/min flow rate. The LA yield was calculated according to the following formula,

$$\text{LA yield } \% = \frac{\text{weight of LA produced (g) x 180.156}}{\text{weight of glucose (g) x 116.11}} \text{ x } 100 \qquad (2)$$

6.1.4. Catalyst Characterization

Thermogravimetric analysis (TGA) of the catalyst supports as well as the optimal catalyst was performed in Perkin-Elmer TGA analyzer (Pyris Diamond TG/DTA) with a N2 gas flow (1.2 L/h) from 30 to 900 °C and a temperature increase rate of 10.0 °C/min. The XRD pattern analysis was carried out with a Cu K α source equipped with an Inel CPS 120 hemispherical detector. The diffraction angle 2θ ranges from 10 to 80°

and the scanning speed was set at 1°/min. The FTIR spectral analysis was performed using FTIR-SHIMADZU (Alpha) with wavenumber ranging from 400 to 4000 cm-1. For determination of the specific surface area, pore size distribution and pore volume, BET and BJH analysis were conducted using Quantachrome Instruments, Nova 4000e. Degassing of the sample was done at 150℃ to remove surface moisture. To determine the total acidity of the catalyst sample NH3-TPD was done using Quantachrome Instruments, TPR win v2.1. XPS analysis was done to determine the binding energy of different elements in the catalyst sample along with their oxidation states. HRTEM analysis was performed in a FEI Titan G2 60 300 transmission electron microscope by fast-tracking voltage of 300 kV. Additionally, the HRTEM images were subjected to analysis using IMAGEJ software to identify and calculate the crystallite lattice spacing. Lastly, to determine the band-gap energy of the prepared photocatalyst UV-VIS DRS analysis was carried out in Perkin Elmer LAMBDA 950 UV–VIS-NIR Spectrophotometer in the range of 200–900 nm. The hydrodynamic particle size of the nano catalyst has been determined by dynamic light scattering using the Zetasizer Nano ZSP (ZEN 5600) from Malvern Instruments Ltd.

6.1.5. Analysis of product

A Waters HPLC system with UV detector (Perkin Elmer 200 series) was used for the chromatographic detection of levulinic acid. The mobile phase was acetonitrile & water (60:40, v/v), with a flow rate of 1 ml/min. The injection volume was 10µl. A Breeze Chromatographic System was used for peak detection and integration (Waters Company, Milford, MA, USA). After equilibrating the column with a mobile phase, the flow rate was maintained at 1.0 mL/min, and 10µL of standard solution subsequently

injected into the chromatographic column. The calibration plots of the corresponding standard constituents were used to calculate the concentrations of the product. At the completion of each experiment, the column was rinsed with same mobile phase for more than 30 minutes.

6.1.6. Life cycle analysis

An environmental life cycle assessment (LCA) of the entire process was carried out to examine its environmental impacts and to compare the efficiency of HRR with CHR systems. The LCA study was performed using the "cradle to gate" methodology, Ecoinvent database 3.9, and the LCA process "ReCiPe Midpoint (H) v1.11" with the aid of OpenLCA software. Fig. 5 explains the system boundaries and process flow diagram for LCA study. The overall process has been broken down to four sub-processes viz. FA treatment, HAp extraction, catalyst preparation and LA synthesis. Each sub-process has been identified by their individual system boundary. The material and utility inputs/outputs has been scaled up in accordance with 1 kg principal outputs of all the sub-processes. The specified LCI data regarding FA treatment, HAp extraction, catalyst preparation and LA synthesis have been listed in Tables 11 – 15.

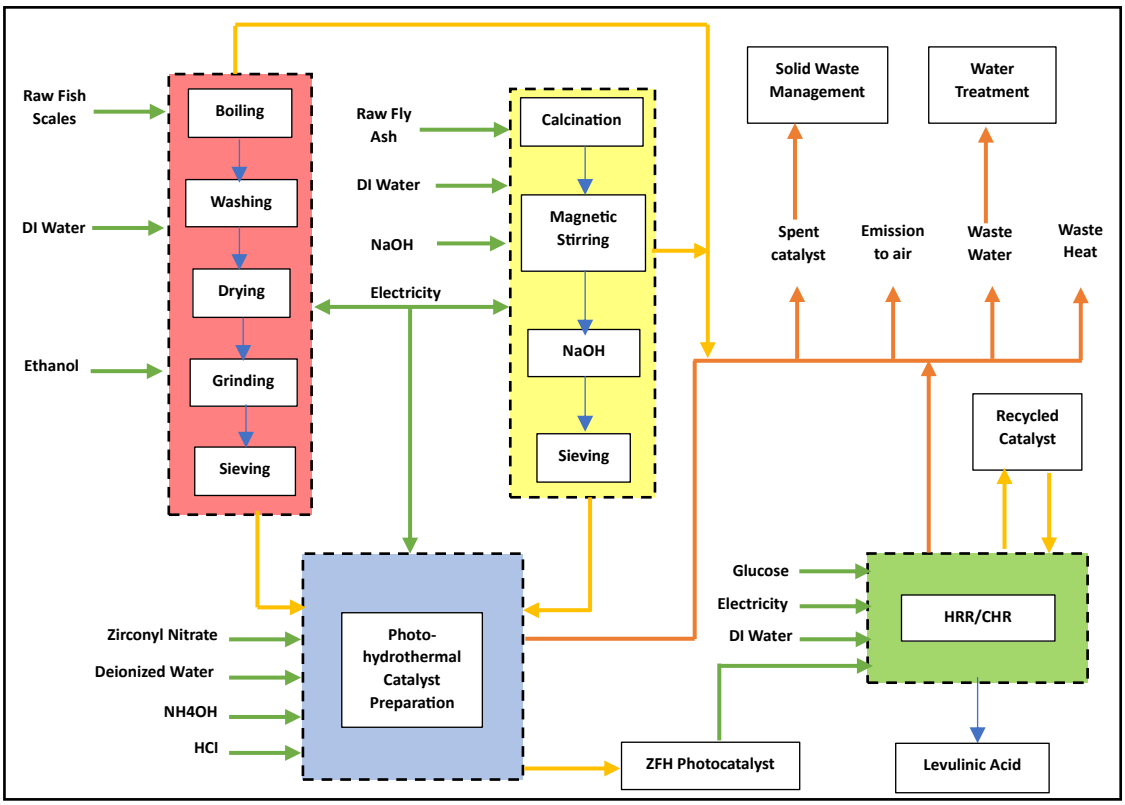

Figure 5. A visual representation depicting the overall process flow and delineating the system boundaries for the LCA study.

6.2. Methods for production of EL from glucose

6.2.1. Design of experiment

To study the simultaneous effects of multiple experimental parameters as well as to determine the optimal operating condition the experimental design has been built in accordance with the Taguchi orthogonal design. The L9 orthogonal array (Table 4) developed in MINITAB-19 software with four independent factors and three levels (Table 3) namely, reaction temperature (X_{tp}), reaction time (X_{tm}), catalyst loading (X_c) and ethanol-to-glucose (E/G) molar ratio (X_v) are considered. The purpose of using Taguchi DOE is that the analysis can be executed within 9 experiments only instead of performing 81 experiments with good accuracy.

To determine the optimal values of the operating parameters corresponding to the maximum value of the response variable the signal to noise ratios (SN) were evaluated according to Eq. 1 and the criteria “larger the better” has been taken into consideration.

$$\frac{S}{N} = -10\log\left(\frac{1}{n}\sum_{k=1}^{n}\frac{1}{Y_k{}^2}\right) \quad \text{..... (3)}$$

Where, 'k' denotes the number of replicates, and 'n' represents the number of trial experiments conducted using various parametric combinations as per Table 4 and Y is the response variable.

Table 3: Experimental factors and levels for ethyl levulinate

Factors	Temperature (℃) X_{tp}	Time (min) X_{tm}	Catalyst loading (wt%) X_c	Ethanol-to-glucose molar ratio X_v
Level 1	100	30	30	15
Level 2	120	45	40	30
Level 3	140	60	50	45

Table 4: L9 orthogonal array experimental matrix at different operating conditions and corresponding mean EL yield (Y) and signal-to-noise (SN) ratio

Runs	X_{tp}	X_{tm}	X_c	X_v	Y	SN
1	100	30	30	15	21.99	26.8445
2	100	45	40	30	25.02	27.9657
3	100	60	50	45	25.71	28.2020
4	120	30	40	45	35.89	31.0995
5	120	45	50	15	39.03	31.8280
6	120	60	30	30	41.55	32.3714
7	140	30	50	30	42.67	32.6025

8	140	45	30	45	48.39	33.6951
9	140	60	40	15	43.66	32.8017

6.2.2. Reactor setup and photocatalytic synthesis

One pot photocatalytic synthesis of ethyl levulinate has been carried out in 500 ml glass vessel (reactor) in presence of hybrid radiation (UV-IR). For optimal reaction condition, 1 g glucose is mixed in 15 ml ethanol (E/G=45) and 30 wt % catalyst (TiO_2 : Amberlyst = 1:2). The reactor is placed inside a square insulated vessel with one UV lamp and one IR lamp mounted in its walls on the opposite ends. At the bottom of the vessel a magnetic stirrer is present on which the reactor assembly is installed. The reaction is conducted under simultaneous exposure of both the lights. The steady temperature could be achieved by varying the intensity of the lights by a regulator. The reaction was carried out at temperature 140 ℃ for 45 mins and at fixed stirring rate of 200 rpm. The reaction temperature is controlled by a PID controller. After completion of the each run in stipulated time the reaction mixture is chilled to room temperature and filtered. After filtration, the excess ethanol is recovered using vacuum distillation. It is then analyzed by HPLC (Perkin Elmer 200 Series) employing a UV detector and water-acetonitrile mixture (60:40 v/v) as mobile phase with 1 ml/min flow rate. The EL yield is calculated according to the following formula,

$$\text{EL yield} = \left[\frac{weight\ of\ EL\ produced\ (g) \times 180.156}{weight\ of\ glucose\ (g) \times 144.17}\right] \times 100\ \% \quad \ldots\ldots\ldots\ldots\ldots\ldots (4)$$

6.2.3. Preparation of fuel blends

The performance of the diesel engine on the basis of brake specific fuel consumption (BSFC), brake power (BP), brake thermal efficiency (BTE), and exhaust gas temperature (EGT) has been studied w.r.t. engine speed. The fuel blend used for the analysis is a diesel-biodiesel-ethyl levulinate mixture abbreviated as BxEy which means it is blend of x% biodiesel and y% EL and the rest diesel i.e., B7E3 is a mixture of 7% biodiesel, 3% EL and 90% diesel. The fuel blends prepared for this study are B0E0, B10E0, B7E3, B6E4 and B5E5. The fuel properties for all blends have been calculated based on the values as reported by Lei et al. [58].

6.2.4. Engine description

A water-cooled, four-stroke engine with a single cylinder (Kirloskar model AV-1) was utilized to assess the quality of fuels (See section 2.4). The engine had a power output of 3.7 kW and a cylinder capacity of 553 cc. In this study, no additional equipment was installed in the engine to enhance fuel atomization or reduce fuel emissions. Instead, the impact on fuel atomization and emission reduction was achieved solely through the use of fuel additives for analysis purposes. To analyze emissions, the engine was operated for 10 minutes to stabilize, after which emission parameters were measured using a gas analyzer.

Chapter 7

RESULTS AND DISCUSSION

7.1. Result and discussion for production of LA from glucose

7.1.1. Statistical analysis of parametric effects

Table 5 shows the ANOVA result corresponding to Table 4. It depicts that reaction temperature is the most significant reaction parameter. Table 6 represents the response table for SN ratios along with the rank and delta values of the parameters (* represents the maximum SN ratio value among the three levels). The optimal reaction conditions viz. temperature, time, precursor loading and glucose amount are found to be 100℃, 120 mins, 20wt% and 3 mmol respectively. An experimental run was taken at these optimal reaction parameters to get a yield of 63.71%. Fig. 6 shows the main effects plot for SN ratios. According to Table 4, temperature is the most significant factor. So, an individual effect of temperature (keeping all other parameters at optimal level) on LA yield has been conducted as shown in Fig. 7. It can be identified that LA yield drops after 115℃ at 76.6%. So, 115℃ is considered the new optimal temperature.

Table 5: Analysis of variance for LA yield.

Source	DF	Adj SS	Adj MS	F-Value	P-Value
Xtp	1	1194.10	1194.10	77.81	0.001
Xtp	1	7.21	7.21	0.47	0.531
Xp	1	4.23	4.23	0.28	0.627
Xg	1	5.63	5.63	0.37	0.577
Error	4	61.39	15.35		
Total	8	1272.56			
R^2	0.95				

Table 6: Response table for signal to noise (SN) ratio.				
Level	X_{tp}	X_{tm}	X_p	X_g
1	29.44	32.17	31.88	32.46
2	32.63	**32.61 ***	**33.16 ***	**32.53 ***
3	**35.24 ***	32.53	32.27	32.31
Delta	5.81	0.44	1.28	0.22
Rank	1	3	2	4
Larger is better				

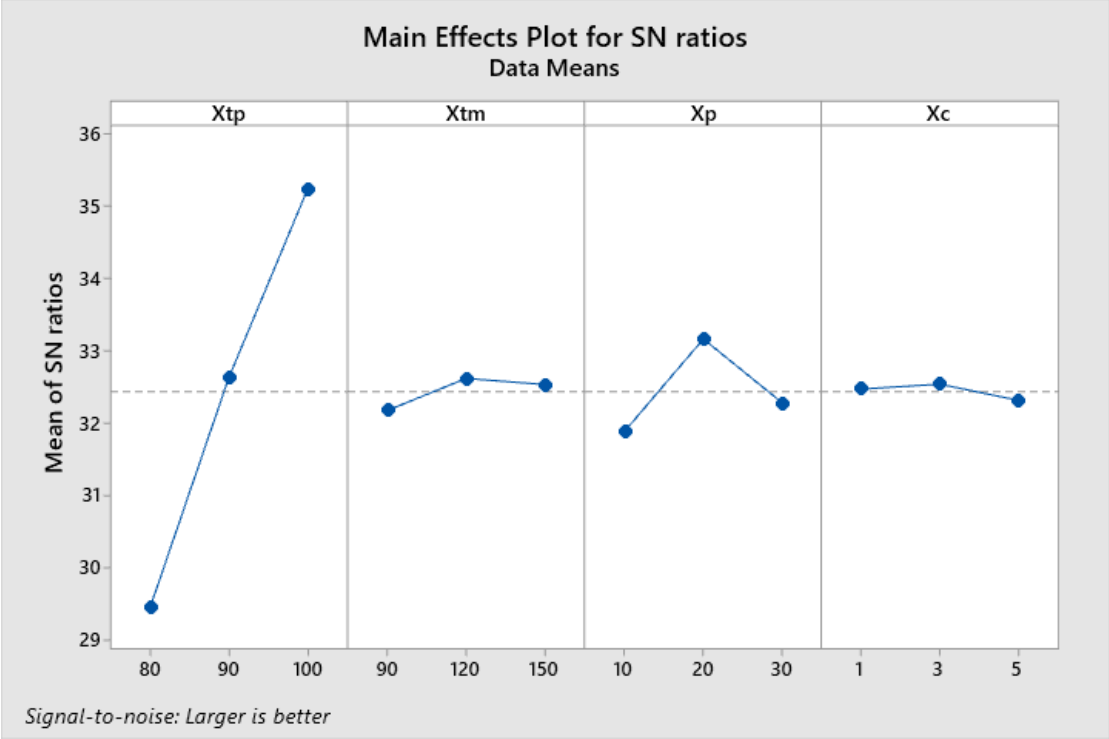

Figure 6. Main effect plot for SN ratios

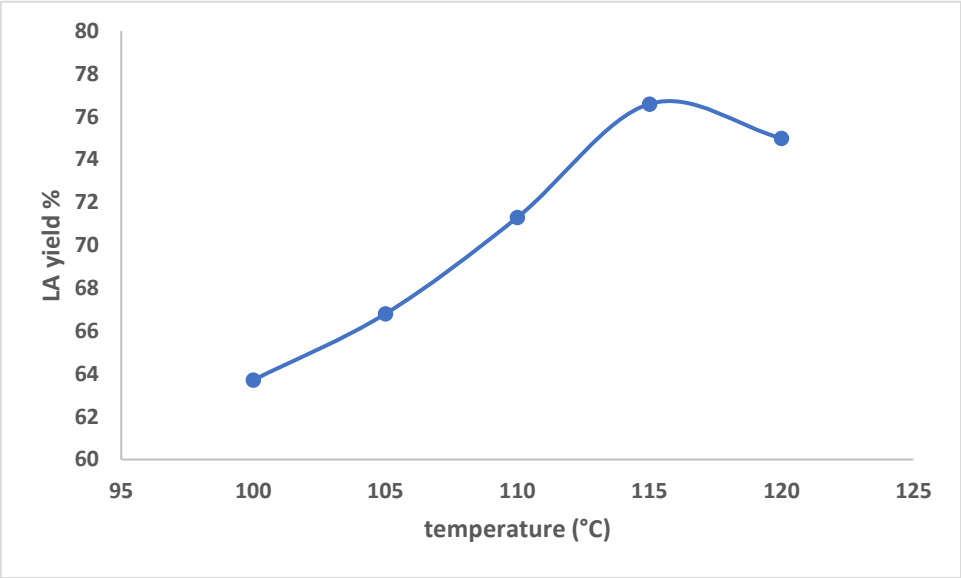

Figure 7. Effect of temperature on LA yield.

The parameter interactive plot has been shown in Fig. 8. From the interaction of Xtp and Xtm it is evident that at 80°C, Y first increases from 90 mins to 120 mins and then decreases from 120 mins to 150 mins. Whereas for 90°C Y almost remains constant. For 100°C Y maximizes at 150 mins. From the interaction between Xp and Xtp it can be inferred that Y gives maxima at 20 wt% for all temperature depicting 20wt% precursor loading as the optimal catalyst loading. The interaction of Xtp and Xg suggests that at optimum temperature the highest Y is achieved at lower glucose amount. The interaction plot of Xtm and Xp depicts maximum Y at optimum Xp. On contrary, the interactions of Xtm and Xg and that of Xp and Xg show decrement in Y at first and then increment at optimal time and glucose amount respectively.

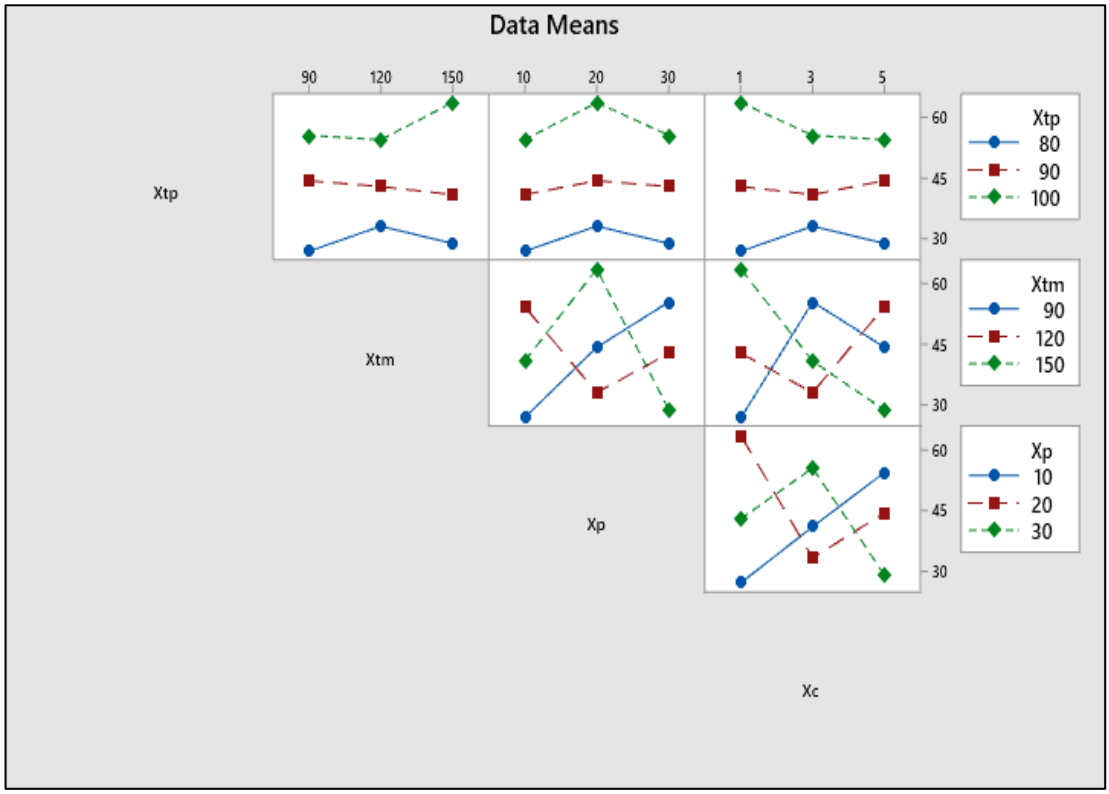

Figure 8. Interaction plot among the process factors for LA yield.

7.1.2. Thermogravimetric Analysis

The Thermo-gravimetric analysis (TGA) graph (Fig. 9) illustrates the weight loss of the uncalcined ZFH2, HAp support and FA support over the heating range of 40–900 °C. The analysis indicates 11.5% weight loss observed in HAp (Hydroxyapatite) is attributed to the evaporation of absorbed water occurring below 200 °C. The sharp fall in weight around 300 °C is attributed to degradation of HAp structure to β-Ca3(PO4)2. No further weight loss is observed after 800 °C. The 3% weight loss for FA support indicates a thermally stable structure. The uncalcined ZFH2 catalyst shows noticeable fall in weight from 100°C-250°C and later around 300°C. The former loss in weight is probably due to evolution of water molecules and nitrogen dioxide from HAp and zirconyl nitrate while the latter weight loss is due to decomposition of HAp to β-

$Ca_3(PO4)_2$ and formation of ZrO_2 [59]. So, the calcination temperature of ZFH2 has been set at 300°C.

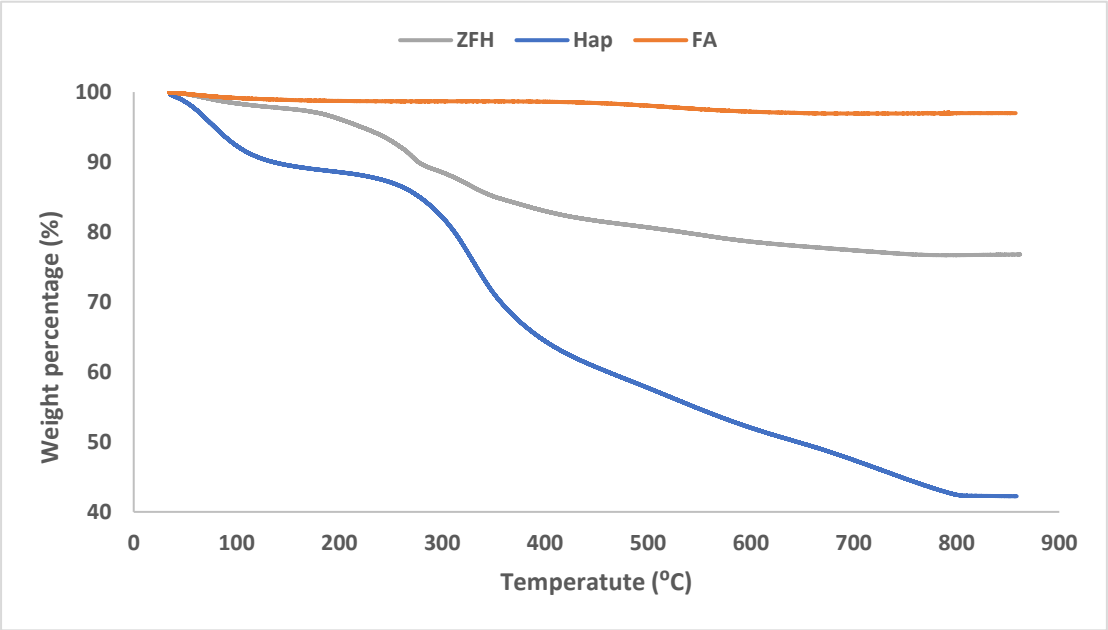

Figure 9. TGA of ZFH2 and supports

7.1.3. X-Ray Diffraction analysis

XRD pattern of all three catalysts under different precursor loadings viz., ZFH1, ZFH2, and ZFH3 are analyzed and showcased in Fig. 10. Prominent peaks of HAp (25.95°, 30.96°, 33.19°, 39.46°) have been identified and matched with JCPDS card no.- 74-0565 [60,61]. Along with HAp, some peaks (35.26°, 36.55°, 40.86°) of DCPA (CaHPO4) are also observed [62]. No peaks of β-Ca3(PO4)2 have been observed in any of the catalyst samples. ZrO_2 peaks (50.16°, 59.95°, 60.65°) have been identified by JCPDS card no. 89-7710 [63]. Furthermore, strong peaks of quartz (26.65°) and mullite (16.45°, 42.54°) have also been identified [64]. The average size of the crystallites was determined using Scherrer's formula, which is expressed as follows: d

= Kλ / βcosθ. In this equation, 'd' represents the mean crystalline size, 'K' is a constant dependent on grain shape (0.9), 'λ' is the wavelength of the incident beam, 'θ' stands for the Bragg reflection angle, and 'β' is the measured broadening of the diffraction line at half its maximum intensity. The calculated average particle sizes of ZrO_2, HAp, quartz, and mullite obtained were 27.42 nm, 39 nm, 66 nm, and 47.5 nm respectively.

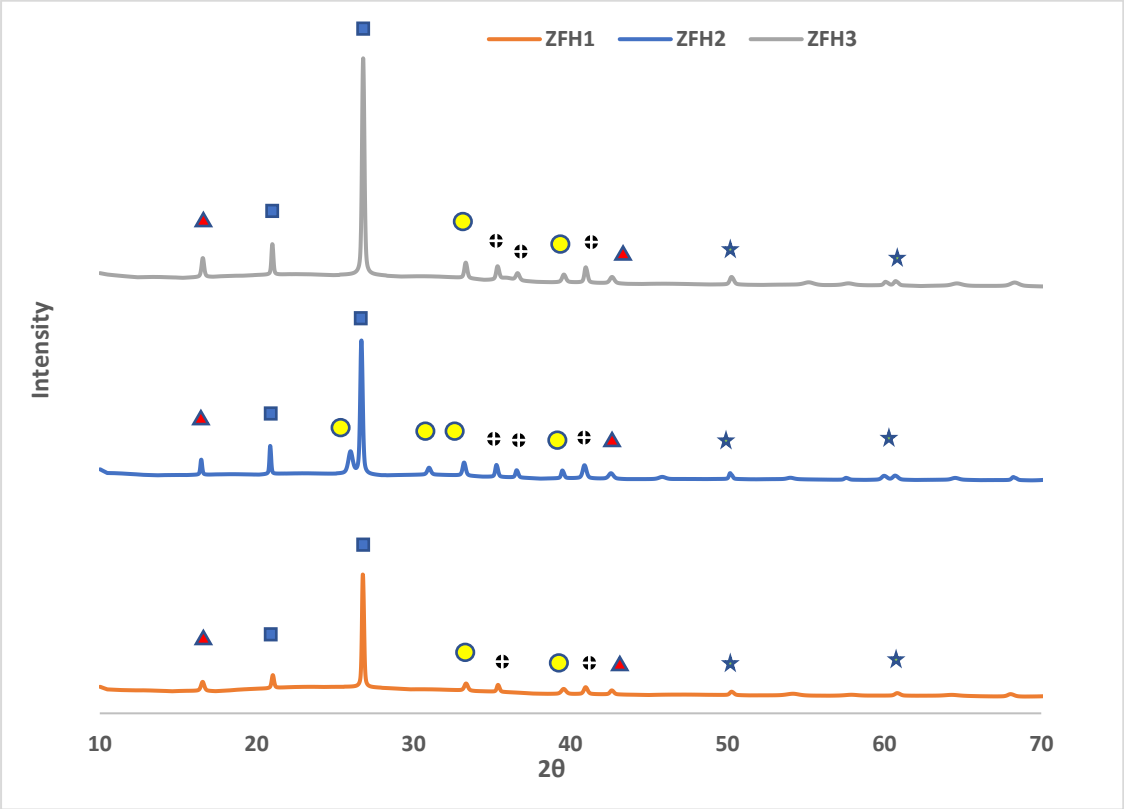

Figure 10. XRD analysis of ZFH samples. ○ *HAp;* ✣ *CaHPO4;* ★ *ZrO_2;* ▲ *mullite;* ■ *quartz.*

7.1.4. Fourier transform infrared spectroscopy

The FTIR result of all the three catalysts under different precursor loadings have been illustratd in Fig. 11. The broad band at 3400 cm-1 represents OH vibration not only due to adsorbed moisture but also from Zr-OH group [65]. This suggested that the prepared ZFH catalysts are hygroscopic in nature. The large amount of moisture adsorbed by the

catalyst corresponds to its superior adsorptive capacity. Whereas, the peak at 1534 cm-1 is due to stretching of OH group [66]. The bands at 1738 cm-1, 1538 cm-1 and 1450 cm-1 are due carbonyl (C=O) group. The peak at 1075 cm-1 is ascribed to Al-O-Si stretching vibration while the peak at 1170 cm-1 is due to Si-O-Si stretch which confirms the presence of aluminosilicate [67]. The 1205 cm-1 and 725cm-1 band correspond to HPO_4^{2-} [65] confirms the presence of $CaHPO_4$. Band at 608 cm-1 confirming the presence of phosphates attributed by the presence of HAp. The peak at 795 cm-1 is assigned to Al-O stretching vibration [67]. While the bands at 578 cm-1 and 430 cm-1 represent Zr-OH [65].

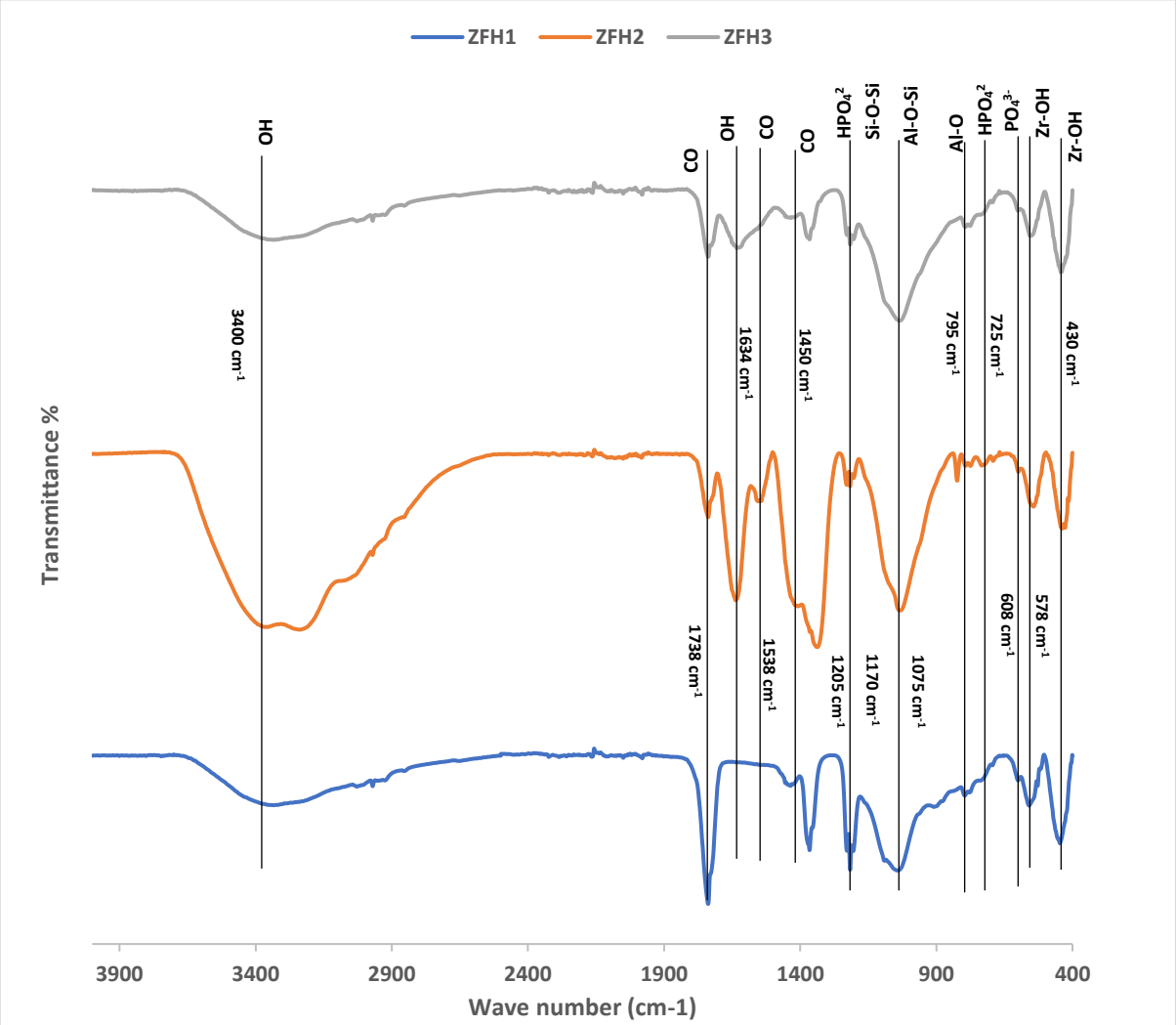

Figure 11. FTIR analysis of ZFH samples.

7.1.5. XPS analysis

The XPS result of ZFH2 is shown in Fig. 12 and the peaks have been identified from standard source [68]. The peaks at 74.2 eV and 102.7 eV represents Al 2p and Si 2p respectively. This confirms the presence of aluminosilicate (SiO2-Al2O3) and quartz in the sample as confirmed by XRD analysis [69]. The peaks at 181.5 eV and 332.5 eV of Zr 3d and Zr 3p ascertains the presence of ZrO_2 [70]. Moreover, Ca 2p and Ca 2s peaks at 347.5 eV and 438.8 eV confirms the presence of HAp [71] and $CaHPO_4$ [72]. Confirmation of the presence of oxygen is supported by the binding energy of O 1s, which measures 531.53 eV. [73].

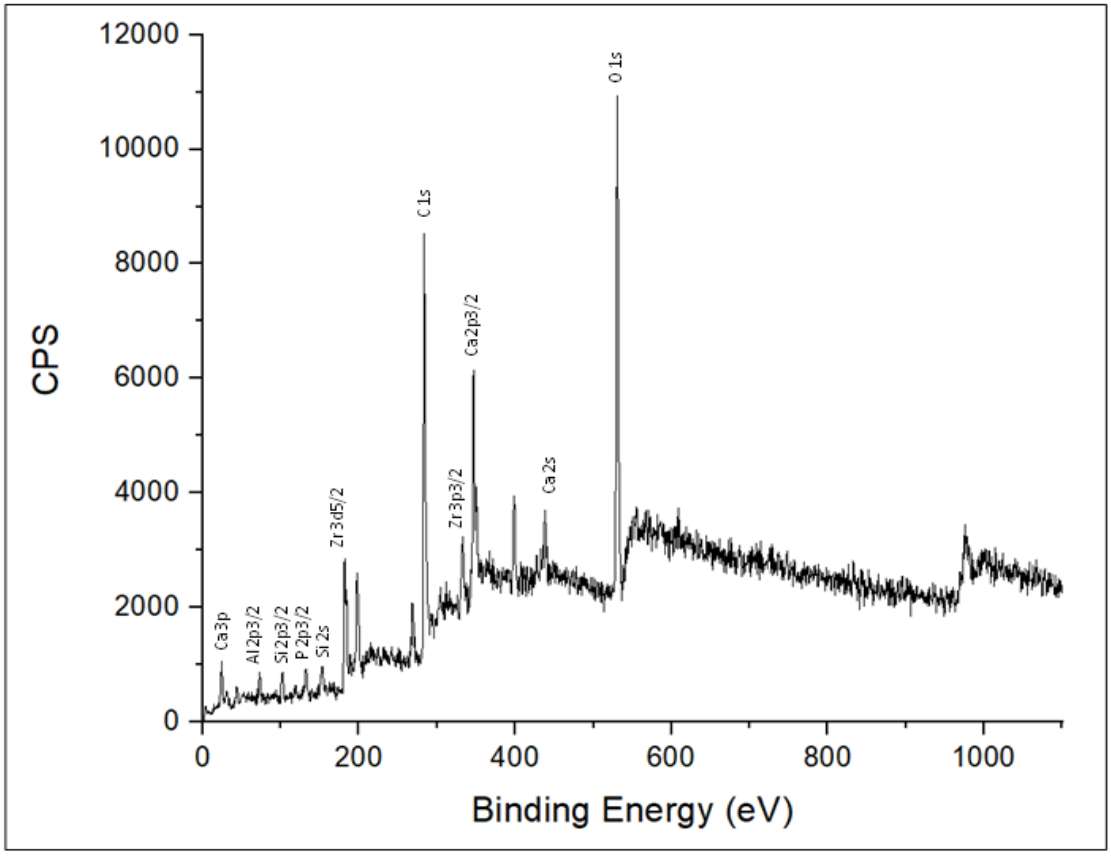

Figure 12. XPS of the optimal catalyst

7.1.6. UV-Vis-NIR Spectroscopy

The UV-VIS-NIR result for ZFH2 has been depicted in Fig. 13. It shows very good absorption in both UV and visible region making the catalyst photosensitive in those wavelengths. The direct band gap energy (Eg=2.15 eV) has been estimated using Tauc plot (Fig. 13 (inside)) as done by Albert et. al [74]. The lower band gap energy - lesser than the commercial TiO_2 catalyst - indicates that ZFH2 is more photo-catalytically efficient catalyst.

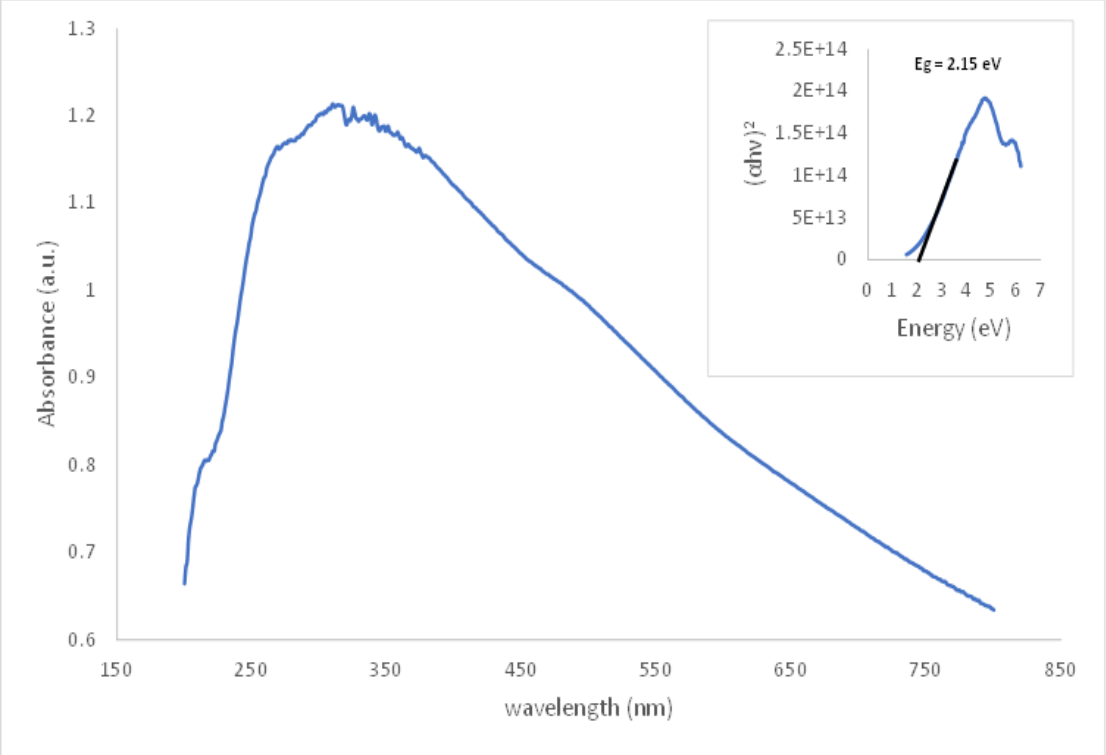

Figure 13. Absorbance spectra of optimal catalyst. (inset) Tauc plot of optimal catalyst

7.1.7. High-resolution transmission electron microscopy

In order to determine the lattice spacing high resolution transmission electron microscopy (HRTEM) analysis of the optimal catalyst has been conducted. Fig 14(a) clearly shows large distribution of spherical ZrO_2 nanoparticles. Fig 14(c) and (d)

shows the lattice spacing of HAp (0.28 nm) [75] and ZrO_2 (0.15 nm) [76] which highly corroborates with the XRD results. Fig. 14(e) displays the EDAX analysis of the optimal catalyst sample along with wt% of the elemental composition.

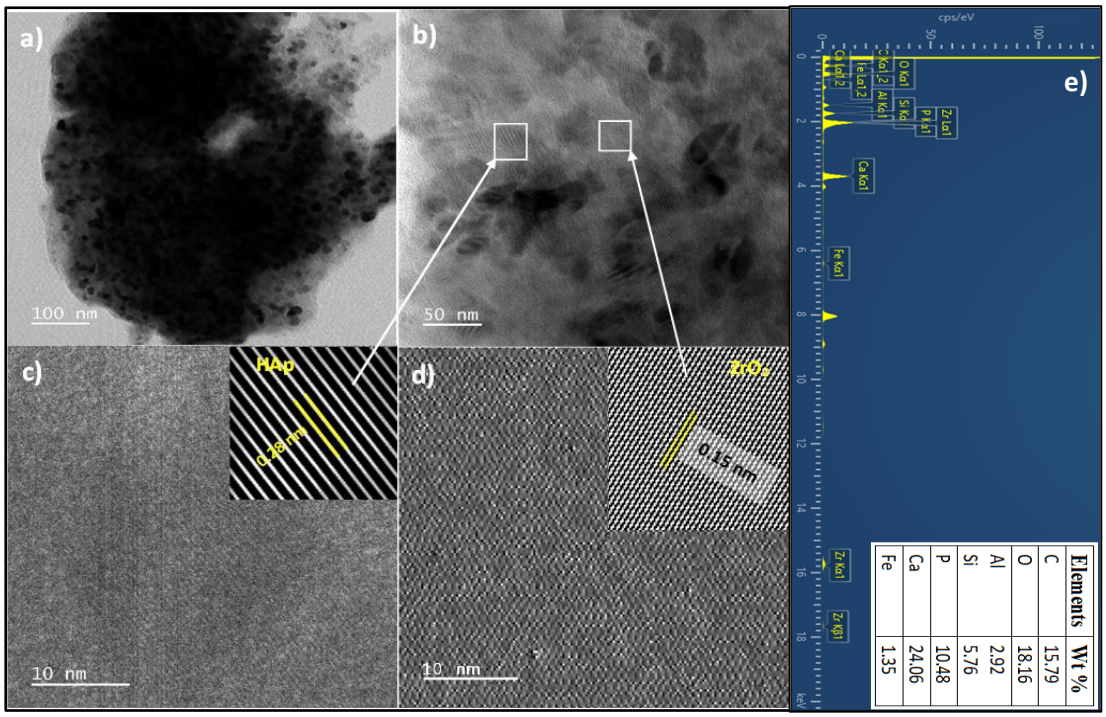

Figure 14. HRTEM and EDAX analysis of ZFH2.

7.1.8. Brunauer-Emmett-Teller (BET) analysis

The result of BET (Brunauer-Emmett-Teller) analysis of the optimal catalyst has been shown in Fig. 15. The specific surface area, pore diameter and pore volume of ZFH1 were 20.924 m^2/g, 0.042 cc/g, 8.029 nm while those for ZFH2 were 62.872 m^2/g, 0.106 cc/g, 6.743 nm and for ZFH3 are 46.032 m^2/g, 0.078 cc/g, 6.778 nm. Such high surface area could be attributed by porous aluminosilicate [77]. It can be deciphered from these data that increase in Zr loading from ZFH1 to ZFH2 had increased the surface area but with further increase in doping the surface area had decreased. This result can be attributed to blocking of pores of the aluminosilicate structure by ZrO_2 molecules. Fig.

16(right) shows the cumulative pore volume vs half pore width plot for ZFH2 sample which indicates the presence of 21.76 % micropore and 78.24 % mesopore.

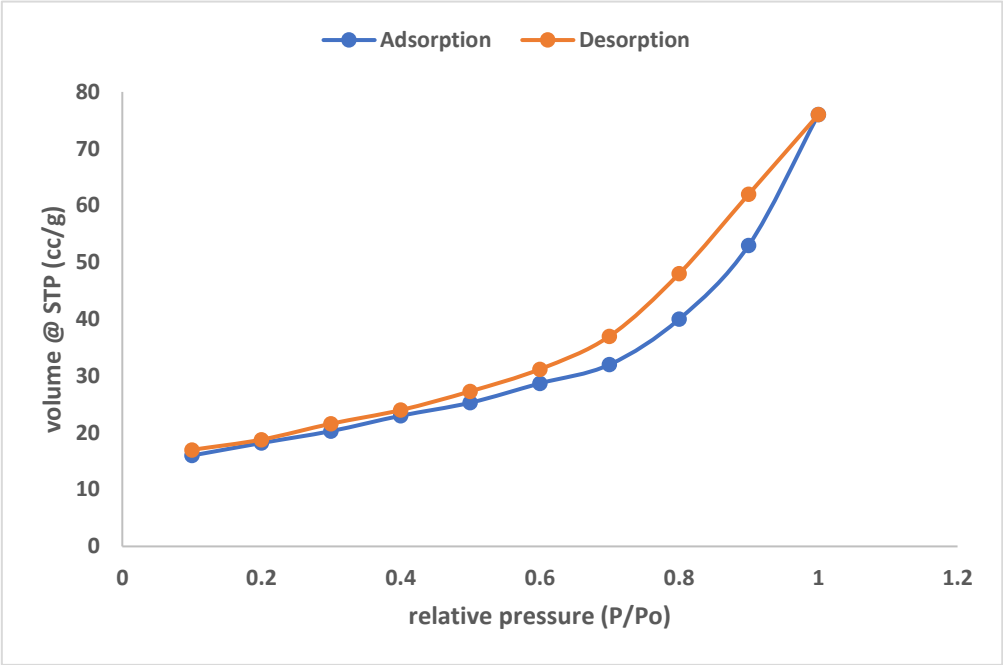

Figure 15. BET isotherm of ZFH2.

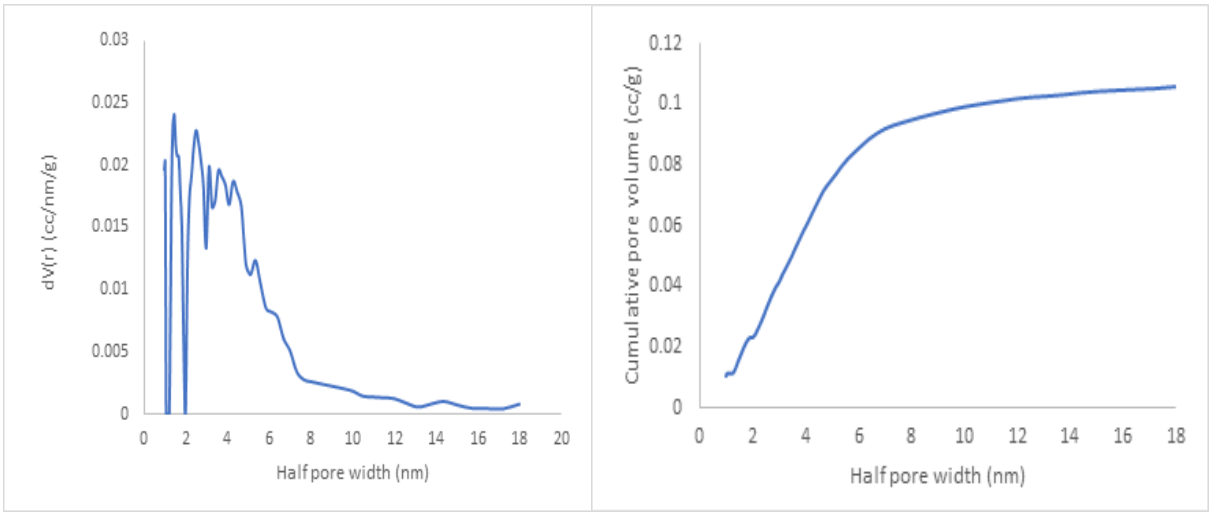

Figure 16. DFT pore-size distribution (left); Cumulative pore volume vs. pore diameter (right) for ZFH2

7.1.9. NH3 TPD analysis

To determine the surface acidity of the catalyst NH3-TPD of ZFH1, ZFH2 and ZFH3 has been performed. It was observed as shown in Fig. 17 that all the catalysts showed a weak peak (signal maxima around 121.4 ℃) and a strong peak (signal maxima around 901.5 ℃). The strong peak may be attributed by Bronsted acidity due to presence of HPO42- [78]. The weak peaks were probably contributed by the Bronsted sites of aluminosilicate [79] as well as Lewis acidic sites of ZrO_2 [42]. The analysis has revealed that ZFH1, which has the lowest Zr loading has lowest acidity of 1.04 mmol/g. It is also observed that ZFH2 (1.52 mmol/g) has slightly higher acidity than ZFH3 (1.506 mmol/g). Thus, it is evident that increasing in Zr concentration from 20 % to 30 % has deteriorating effect on catalyst performance. The reason behind this observation might be inclusion of Zr4+ in HAp structure thus creating a charge imbalance which is compensated by conversion of OH- ions to O2-. This comes at a cost with reduction in P-OH intensity as confirmed by FTIR analysis. P-OH is the source of Bronsted acidity, so reduction in its intensity dictates the reduction in total acidity of ZFH3 sample [80].

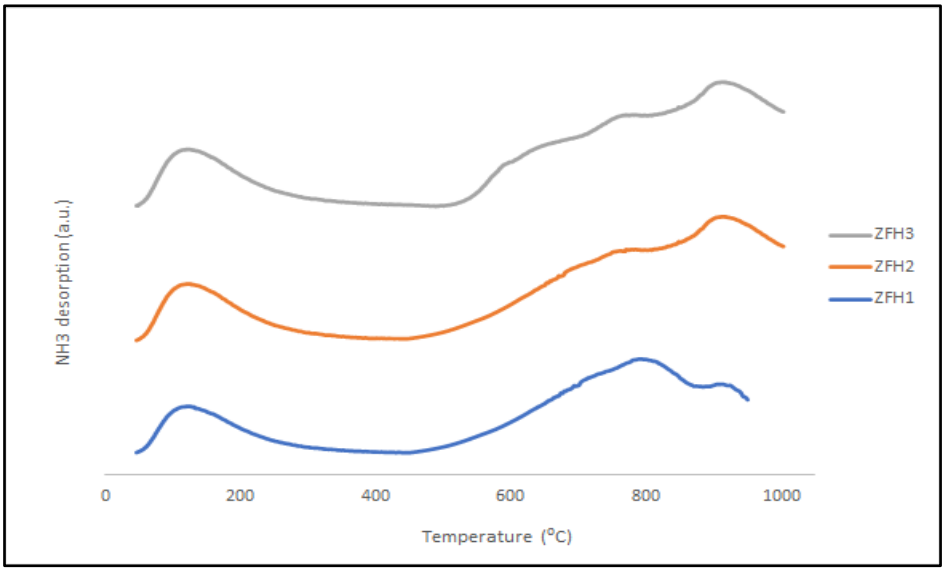

Figure 17. NH3-TPD of the synthesized catalysts.

Table 7: Morphology and acidity of the prepared catalyst samples.				
Catalyst	**BET SSA m^2/g**	**Pore volume cc/g**	**Pore diameter nm**	**Total acidity mmol/g**
ZFH1	20.924	0.042	8.029	1.04
ZFH2	62.872	0.106	6.743	1.52
ZFH3	46.032	0.078	6.778	1.506

7.1.10. Particle size analysis using dynamic light scattering

The particle size of prepared catalyst sample has been explored using DLS method. Fig. 18 shows the number size distribution of the sample and the average particle diameter reported is found to 78.82 nm with a standard deviation of 8.34 nm. The size of the particles as reported by DLS method be larger than that calculated from XRD result. This can be understood because in DLS the nano particles are dispersed in solution which forms a hydration layer around the particles and thus, the effective particle size increases [81].

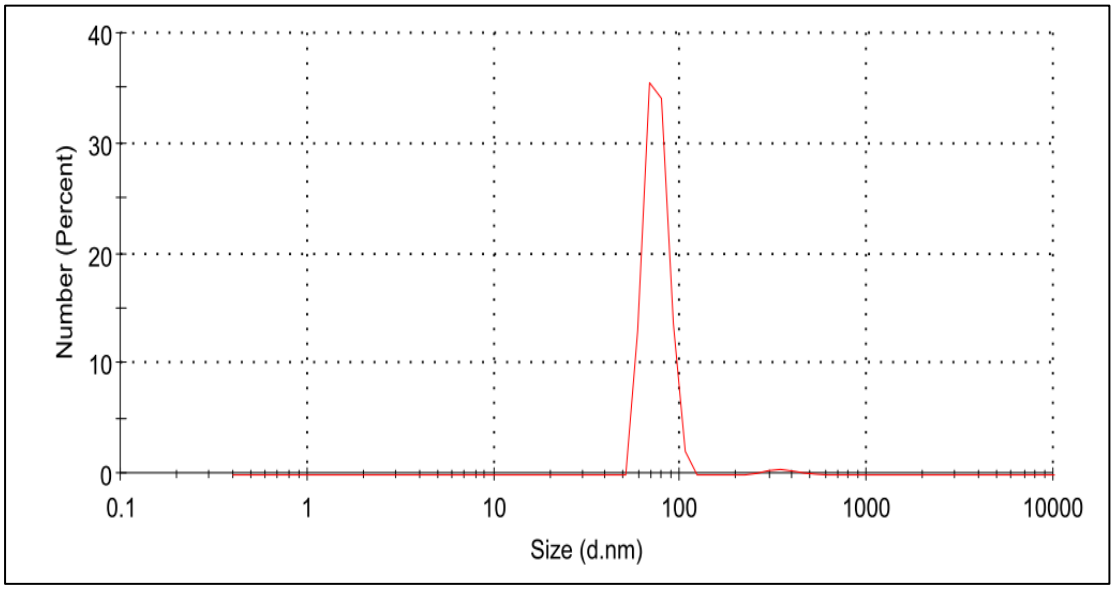

Figure 18. Number size distribution of ZFH2.

7.1.11. Effect of different radiation

The performance of the catalyst has been studied in different radiation systems at optimal reaction conditions as shown in Table 8. The blank run without any radiation and catalyst gives little to no yield. In the presence of the catalyst, the UV-only system gives a very little yield of 12.53% while the FIR-only system gives a yield of 18.67%. In the case of a hybrid radiation system, in the absence of ZFH2 catalyst, the reaction does not yield any product but in the presence of the catalyst, a significantly high LA yield of 76.6% has been observed. Thus, these observations confirmed that ZFH2 plays a vital role in the reaction but its photocatalytic activity is fully realized by the synergistic effect of UV and FIR radiations. The reason is probably because the photocatalyst is UV responsive as confirmed by the UV-VIS-NIR result while FIR facilitated the reaction with its capacity to bend and stretch water molecules involved in LA formation (see Fig. 19).

Table 8: LA yield in different radiation systems

Radiation system	**No radiation without ZFH2**	**No radiation with ZFH2**	**UV radiation with ZFH2**	**FIR radiation with ZFH2**	**Hybrid radiation (UV+FIR) without ZFH2**	**Hybrid radiation (UV+FIR) with ZFH2**
LA yield	Nil	23.7%	12.53%	18.67%	Nil	76.6%

7.1.12. Reaction mechanism for LA synthesis

The Zr (IV) of ZrO_2 acts as Lewis acidic sites which helps in glucose isomerization to fructose according to Joshi et al. [42]. The Bronsted acidic sites (denoted as H+ in Fig. 19) contributed by CaHPO42- as well as aluminosilicate promotes conversion of fructose to HMF through successive dehydration. HMF being a very reacting compound rehydrates and dehydrates itself in presence of Bronsted acidic sites to ultimately forming levulinic acid [82].

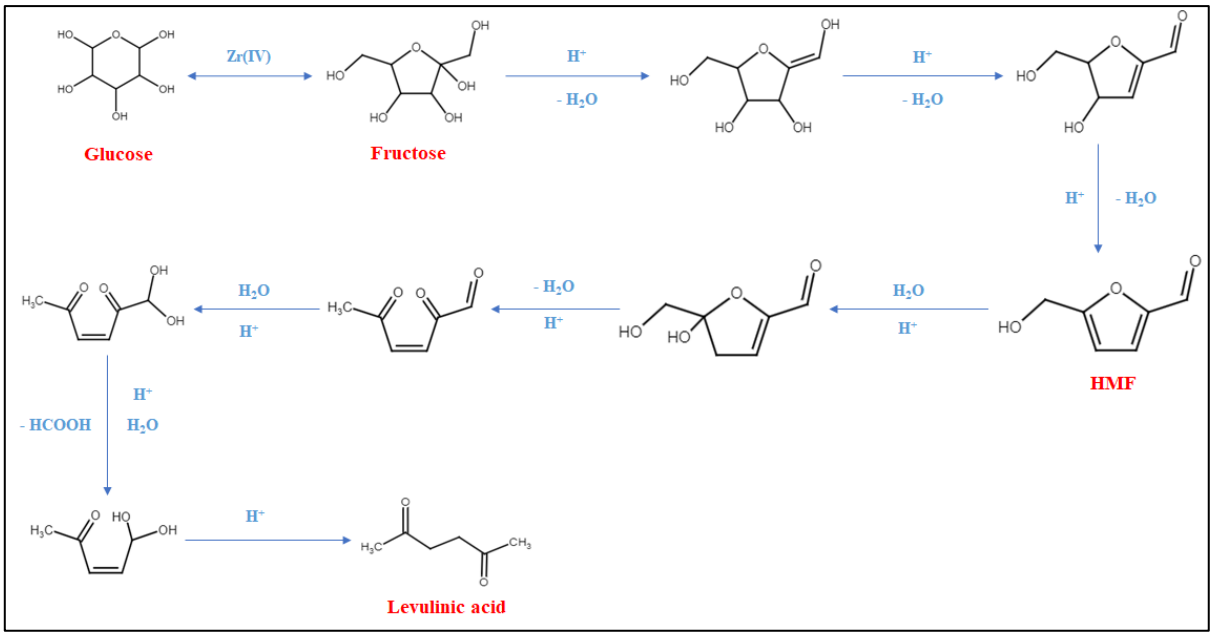

Figure 19. Reaction mechanism for glucose conversion to levulinic acid.

7.1.13. Catalyst Reusability

To study the catalyst reusability and regeneration, five successive runs have been taken as shown in Fig. 20. After completion of run 1 the used catalyst was filtered and dried and then used again in run 2 directly without calcination. As a result, LA yield at run 2 showed a decrease of 3%. So, after completion of run 2, the used catalyst was filtered and calcined at 200°C. Subsequently, the LA yield at run 3 again increased. The next successive runs were taken with the used catalyst calcined between each run and it was observed that the LA yield remains almost constant. This suggested that due to the strong hygroscopic nature of ZFH2, there was a partial drop in catalytic activity by the adsorbed water molecules which was revamped by calcining the catalyst after each run. Also, since there was no fall in LA yield in later runs it can be concluded that there was no leaching in our prepared catalyst.

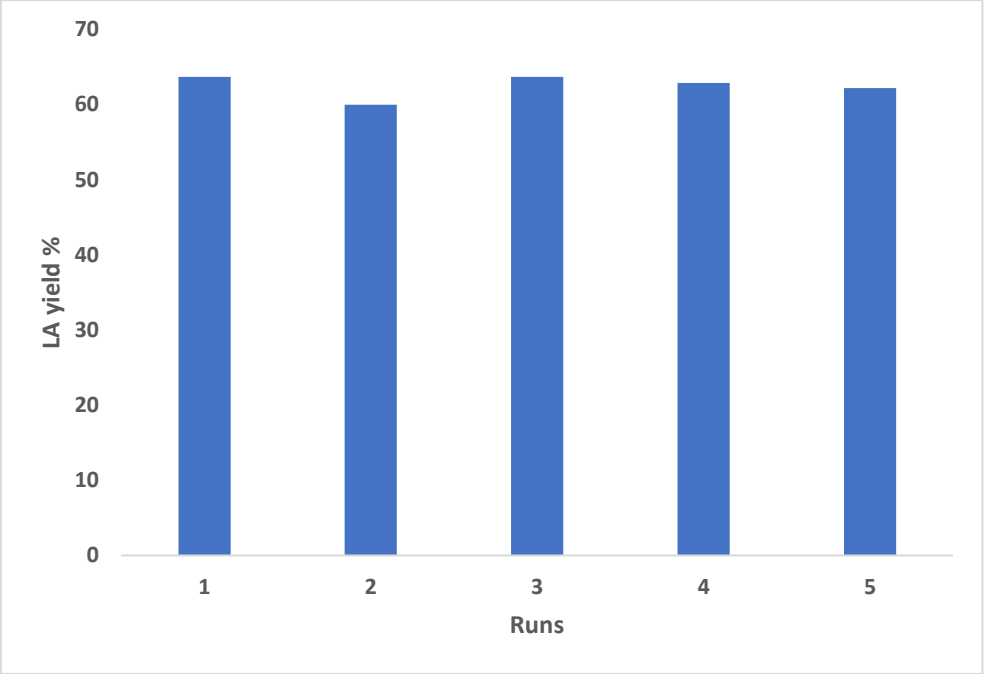

Figure 20. Catalyst reusability study.

Table 9: Comparative study of LA production in terms of reaction conditions.

Feedstock	Catalyst	Reaction conditions	LA yield	Remarks	Ref.
glucose	GaHPMo	175℃, 10 h	56%	• Severe reaction condition especially the time factor is too high. • Traditional heating so high environmental impact.	83
glucose	$CrCl_3$/HY	160℃, 3 h	62%	• Severe reaction condition especially the time factor is too high. • Traditional heating so high environmental impact.	84
glucose	H_2SO_4	170℃, 0.5 h	26.1%	• Use of mineral acids so difficulty in separation and high environmental impact. • Microwave (MW) assisted reaction. • Reaction temperature is very high. • Low yield. • Increasing reaction time causes humin formation.	85
	HCl		31.4%		
glucose	TiO_2	150℃, 4 h	60%	• UV radiation applied. • Higher reaction temperature and time. • Low yield.	86
Glucose	**ZFH2**	**115℃, 2 h**	**76.6%**	• UV-FIR hybrid radiation applied.	**Present study**

				• Lower reaction temperature and time. • Higher yield. • More energy efficient. • Lower environmental impact.	

Table 10: Comparative study of LA production in terms of catalyst property.

Feedstock	Catalyst	Catalyst property	Reaction conditions (Temp, press, time, catalyst conc)	LA yield	Ref.
Glucose	ZrC+Amberlyst-15 (1:1 w/w)	Basicity: 0.2 mmol/g BET SSA: NA	120℃, 12 h, 100 wt%	17%	[87]
Glucose	SO_4^{2-}/ZrO_2	Acidity: 0.862 mmol/g BET SSA: 6.131 m^2/g	160 °C, 2 h, 100 wt%	29.68%	[88]
Glucose	ZRP zeolite	Acidity: 2.33 mmol/g BET SSA: NA	180 °C, 1.7 MPa, 8 h, 75 wt%	35.8%	[89]
glucose	**ZFH2**	**Acidity: 1.52 mmol/g BET SSA: 62.872 m^2/g**	**115 °C, 2 h, 20 wt%**	**76.6%**	**Present study**

7.1.14. Life cycle impact assessment

The results of the LCA utilizing ReCiPe Midpoint (H) v1.11 are depicted in Fig. 21. The LCA data for different processes are tabulated in Table 11 – 15. The findings showed that the main midway impact indicators for all three system borders comprised global warming (GW), fossil resource scarcity (FRS), terrestrial ecotoxicity (TE), water consumption (WC), and human toxicity (HT). The ZFH2-catalyzed photocatalytic conversion of glucose in HRR resulted in fewer impacts in all categories in comparison to catalytic conversion in CHR, which compares the environmental effects of catalytic reaction in both types of reactors. The GW was reduced by 59 %, FRS by 70.66 % & TE by 65 % by using HRR over CHR. Additionally, Fig. 22 indicates that the catalyst preparation step contributes the highest to GW (38.94 %) and FRS (38.75 %) mainly due to higher electricity consumption whereas the HRR reaction step is the main

contributor to WC (79.83 %) and HT (47.30 %). FA treatment required transportation of raw fly ash from far and remote power stations, thus, involving diesel consumption which contributes to TE (36.73 %).

The energy required to achieve an LA yield of 76.6% from glucose in HRR (450 W, 2 h) is 3.24 MJ, while to produce 58% LA in CHR (500 W, 4 h), the energy required was 7.2 MJ. Hence, the HRR is 120% more energy efficient than CHR. Also, a cost analysis is conducted for optimal ZFH catalyst preparation and levulinic acid production. The estimated cost of 1 kg ZFH2 is INR 806.58 whereas that of levulinic acid is INR 5648.46 (commercially available levulinic acid costs INR 7577.50 per kg).

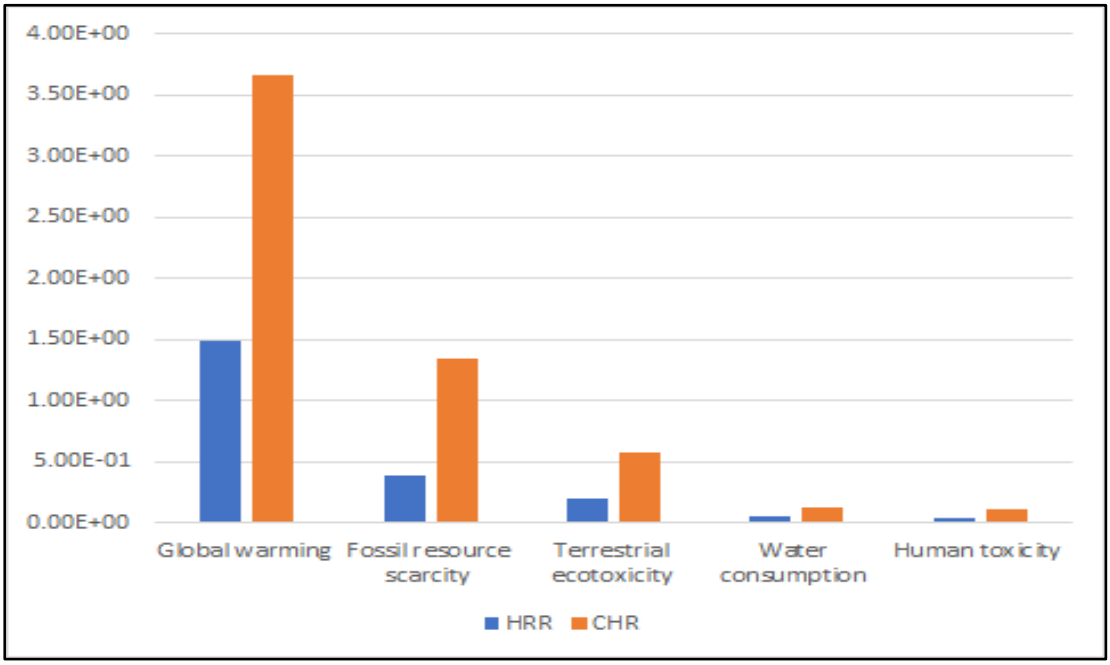

Figure 21. Comparative environmental impacts of HRR and CHR

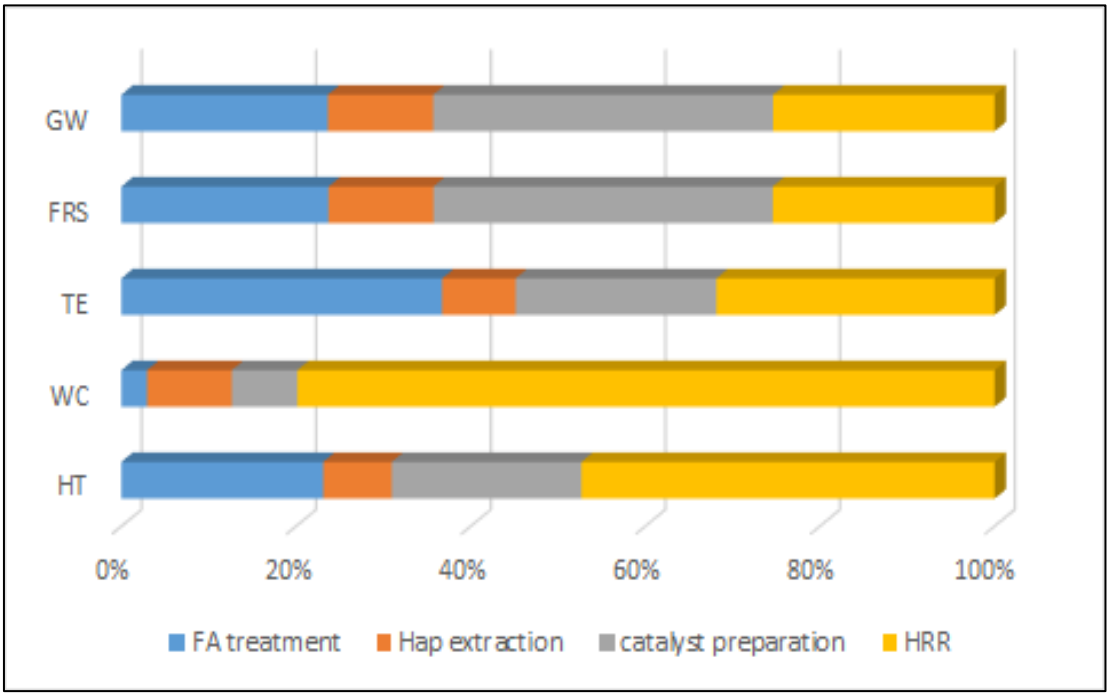

Figure 22. Relative percentage contribution of different sub processes for HRR

Table 11: LCI data for preparation of 1 kg Fly ash support				
Category	**Flow**	**Value**	**Unit**	**Source**
Energy Input	Energy consumed		KWh	Ecoinvent v3.9
	For calcination	2		Ecoinvent v3.9
	For magnetic stirring	0.05		Ecoinvent v3.9
	Total energy	**2.05**		Ecoinvent v3.9
Material Input	Fly ash	1.0097	Kg	Ecoinvent v3.9

	NaOH	0.2	Kg	Ecoinvent v3.9
	DI Water	5	kg	Ecoinvent v3.9
Emissions to air	Waste Heat	2.05	kWh	Ecoinvent v3.9
	Particulates <10µm	0.0097	Kg	Ecoinvent v3.9
Transports	Fly ash	74	Kg*Km	Ecoinvent v3.9
Output	Fly ash support	1	kg	Created

Table 12: LCI data for preparation of 1 kg Hap support

Category	**Flow**	**Value**	**Unit**	**Source**
Energy Input	Energy consumed		KWh	Ecoinvent v3.9
	For Boiling	0.25		
	For Oven drying	0.8		
	Total energy	**1.05**		
Material Input	Fish scale	1.0114	kg	Ecoinvent v3.9
	DI Water	4	kg	Ecoinvent v3.9

	Ethanol	1.4	kg	Ecoinvent v3.9
Emissions to air	Waste Heat	1.05	KWh	Ecoinvent v3.9
	Water Vapour	0.296	Kg	Ecoinvent v3.9
	Particulates <10µm	0.0114	Kg	Ecoinvent v3.9
Transports	Ethanol	0.00005	Kg*Km	Ecoinvent v3.9
	DI Water	0.00032	Kg*Km	Ecoinvent v3.9
Waste of Materials	Waste Water	3.704	Kg	Ecoinvent v3.9
	Ethanol	1.4	kg	Ecoinvent v3.9
Output	HAp	1	Kg	Created

Table 13: LCI data for preparation of 1 ZFH2 catalyst

Category	**Flow**	**Value**	**Unit**	**Source**
Energy Input	FIR radiation	0.5	KWh	Ecoinvent v3.9
	Calcination	1.35	KWh	Ecoinvent v3.9

	Oven drying	0.3	KWh	Ecoinvent v3.9
	Total	2.15	kWh	Ecoinvent v3.9
Material Input	FA support	0.4	kg	Ecoinvent v3.9
	Hap support	0.4	kg	Ecoinvent v3.9
	Zirconyl nitrate	0.2	Kg	Ecoinvent v3.9
	DI Water	0.8	kg	Ecoinvent v3.9
	HCl	0.66	kg	Ecoinvent v3.9
	Ammonium Hydroxide	0.028	kg	Ecoinvent v3.9
Emissions to air	Waste Heat	2.15	KWh	Ecoinvent v3.9
Transport	Zirconyl nitrate	0.000088	Kg*Km	Ecoinvent v3.9
	HCl	0.0000655	Kg*Km	Ecoinvent v3.9
	Ammonium Hydroxide	0.0000013	Kg*Km	Ecoinvent v3.9
Output	ZFH2 catalyst	1	Kg	Created

Table 14: LCI data for preparation of 1 kg Levulinic acid in HRR

Category	Flow	Value	Unit	Source
Energy Input	Electricity Consumption			
	For heating	0.4	kWh	Ecoinvent v3.9
	Stirring	0.028	kWh	Ecoinvent v3.9
	Vacuum evaporation	0.1	kWh	Ecoinvent v3.9
	Total	0.528	kWh	Ecoinvent v3.9
Material Input	Glucose	2.46	Kg	Ecoinvent v3.9
	Distilled water	45	kg	Ecoinvent v3.9
	ZFH2 catalyst	0.492	Kg	Ecoinvent v3.9
Emission to air	Waste heat	0.528	KWh	Ecoinvent v3.9
Waste of Material	Waste water	4.5	kg	Ecoinvent v3.9
Output	Levulinic acid	1	kg	Created

Table 15: LCI data for preparation of 1 kg Levulinic acid in CHR				
Category	**Flow**	**Value**	**Unit**	**Source**
Energy Input	Electricity Consumption			
	For heating	0.6	kWh	Ecoinvent v3.9
	Stirring	0.028	kWh	Ecoinvent v3.9
	Vacuum evaporation	0.1	kWh	Ecoinvent v3.9
	Total	0.928	kWh	Ecoinvent v3.9
Material Input	Glucose	7.046	Kg	Ecoinvent v3.9
	Distilled water	120	kg	Ecoinvent v3.9
	ZFH2 catalyst	1.4092	Kg	Ecoinvent v3.9
Emission to air	Waste heat	0.928	KWh	Ecoinvent v3.9
Waste of Material	Waste water	12	kg	Ecoinvent v3.9
Output	Levulinic acid	1	kg	Created

7.2. Results and Discussion for production of EL from glucose

7.2.1. Statistical analysis of parametric effects on EL yield

Table 16 shows the ANOVA result corresponding to Table 4. It depicts that reaction temperature is the most significant reaction parameter. Table 17 represents the response table for SN ratios along with the rank and delta values of the parameters (* represents the maximum SN ratio value among the three levels). The optimal reaction condit ions viz. temperature, time, feed to catalyst loading and E/G are found to be 140°C, 45 mins, 30wt% and 45 respectively. An experimental run was taken at these optimal reaction parameters to get a yield of 49.33%. Fig. 23 shows the main effects plot for SN ratios.

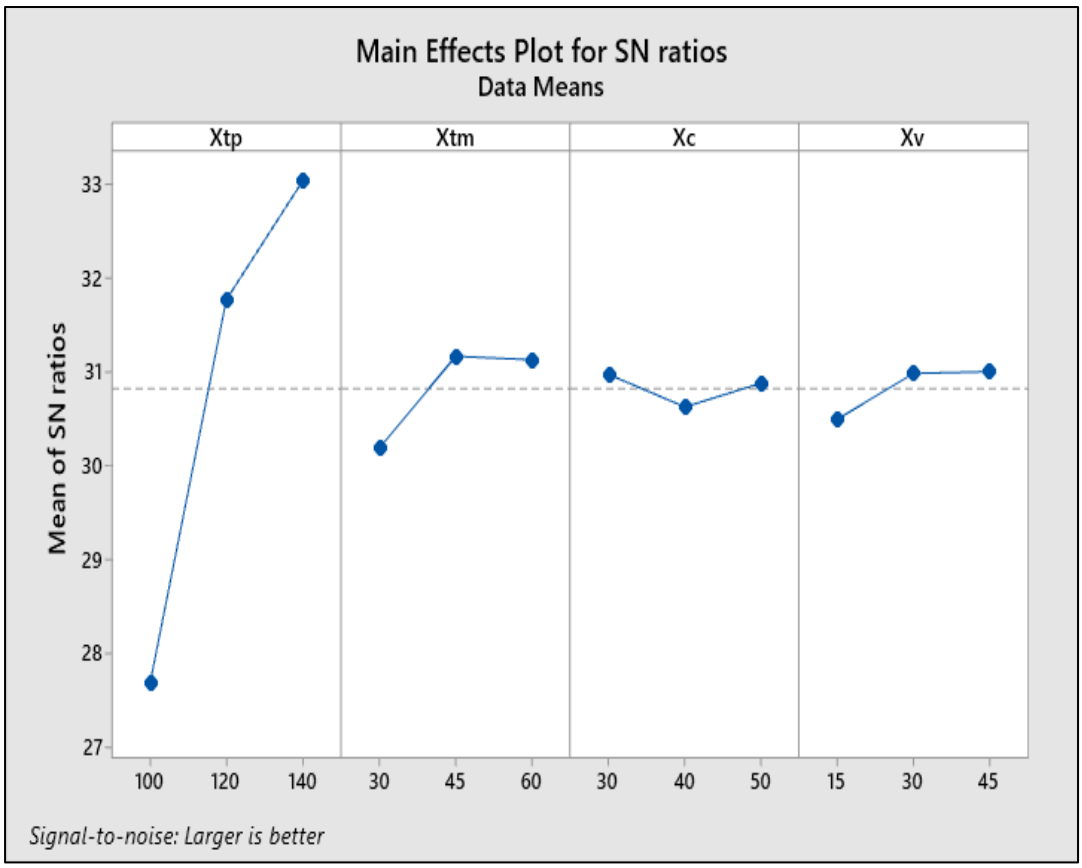

Figure 23. Main effects plot for SN ratios.

Table 16: Analysis of variance for EL yield					
Source	**DF**	**Adj SS**	**Adj MS**	**F-Value**	**P-Value**
Xtp	1	640.667	640.667	48.63	0.002
Xtm	1	17.923	17.923	1.36	0.308
Xc	1	3.405	3.405	0.26	0.638
Xv	1	4.699	4.699	0.36	0.583
Error	4	52.702	13.175		
Total	8	719.396			

Table 17: Response table for signal to noise (SN) ratio				
Level	**X_{tp}**	**X_{tm}**	**X_c**	**X_v**
1	27.67	30.18	**30.97***	30.49
2	31.77	**31.16***	30.62	30.98
3	**33.03***	31.13	30.88	**31.00***
Delta	5.36	0.98	0.35	0.51
Rank	1	2	4	3

The parameter interactive plot has been shown in Fig. 24. From the interaction of Xtp and Xtm it is evident that at 140°C, Y first increases from 30 mins to 45 mins and then decreases from 45 mins to 60 mins probably due to humin and other by-product formation. Whereas for both 120°C and 100°C Y increases steadily with time. From the interaction between Xc and Xtp it can be inferred that Y gives maxima at 30 wt% as temperature increases depicting 30wt% catalyst loading as the optimal catalyst loading. The interaction of Xtp and Xv suggests that at optimum temperature the highest Y is achieved at higher ethanol volume. The interaction plot of Xtm and Xc depicts maximum Y at lower catalyst loading.

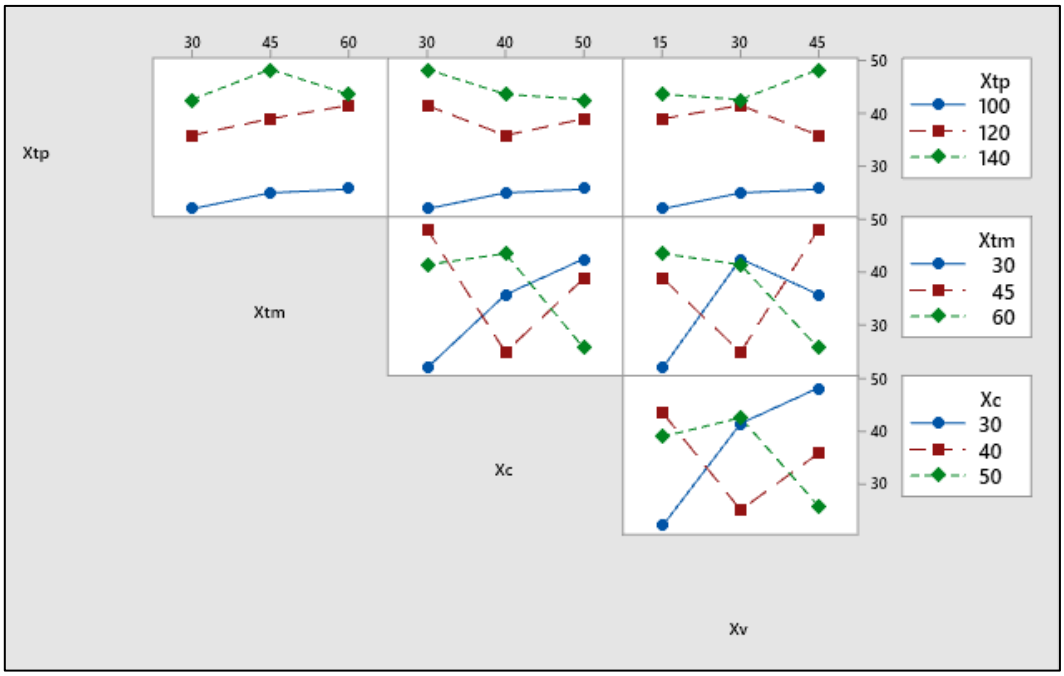

Figure 24. Interaction plot among the process factors for EL yield.

7.2.2. Effect of different catalyst systems on EL yield

The effect on yield of various products have been studied under optimal reaction conditions in various catalyst systems. In Fig. 25 the yields of LA and EL have been plotted for TiO_2, Amberlyst-15+TiO_2, Amberlyst-16+TiO_2, Amberlyst-36+TiO_2 with

glucose as feed. It has been observed that using TiO_2 as the only catalyst is proved to ineffective which gives very negligible product yields. For the second catalytic system of Amberlyst-15+TiO_2 both the LA and EL yields rose to 22.47% and 15.69% respectively implying Amberlyst plays a vital role as Bronsted acid for production of LA and EL. For the second catalytic system of Amberlyst-16+TiO_2 all the yields of the products significantly increase with LA being the highest product. But for the catalytic system of Amberlyst-36+TiO_2 the EL yield surpasses that of LA depicting Amberlyst-36 variant to be the best among all.

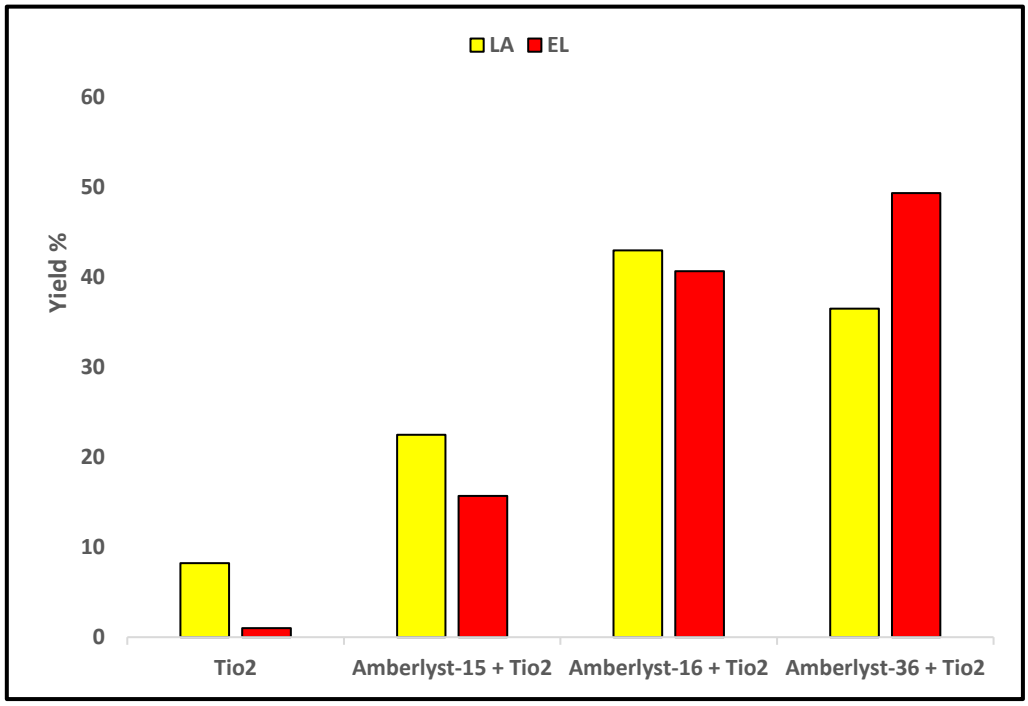

Figure 25. Effect of different catalyst system on product yield.

Reaction conditions: glucose 1g, temperature 140 °C, time 45 mins, catalyst loading 30 wt% and ethanol-to-glucose ratio 45, rotational speed 200 rpm.

7.2.3. Effect of ethanol-to-glucose molar ratio and rotational speed on EL yield

To address the unreacted LA in the system the ethanol-to-glucose ratio has been increased at optimal condition. From Fig. 26 it is evident that with increase in ethanol quantity the EL yield increases till ethanol-to-glucose ratio reaches 90 and then the yield

remains constant at 64%. Next, to address any external mass transfer limitation the rotational speed is varied. Fig. 27 suggests that after 350 rpm the yield becomes constant at 76.08%.

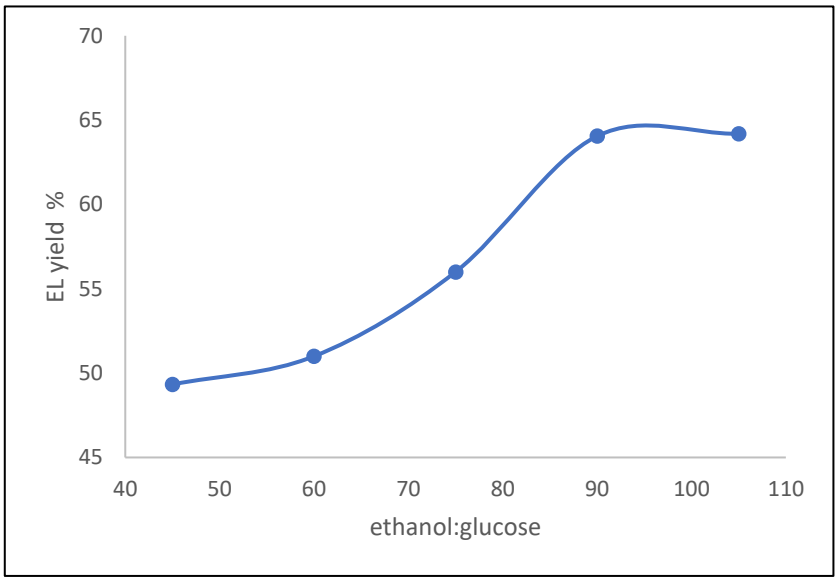

Figure 26. Effect of ethanol-to-glucose ratio on EL yield.

Reaction conditions: glucose 1g, temperature 140 ℃, catalyst loading 30 wt% and rotational speed 200 rpm.

7.2.4. Effect of different radiation systems on EL yield

The performance of the catalyst has been studied in different radiation systems at optimal reaction condition as shown in Table 5. The blank run with no catalyst gives little to no yield. Conventional electrical heating gives a yield of only 23.56%. The UV only system gives very little yield of 15.88% while the IR only system gives a yield of 20.56%. But in case of hybrid radiation system significantly high EL yield of 76.08% has been perceived. The synergistic effect of UV and FIR radiations is probably because the photocatalyst TiO_2 is UV responsive which helps in glucose isomerization to fructose while IR facilitate the reaction with its capacity to bend and stretch water molecule required for EL formation (see Fig. 28) [90].

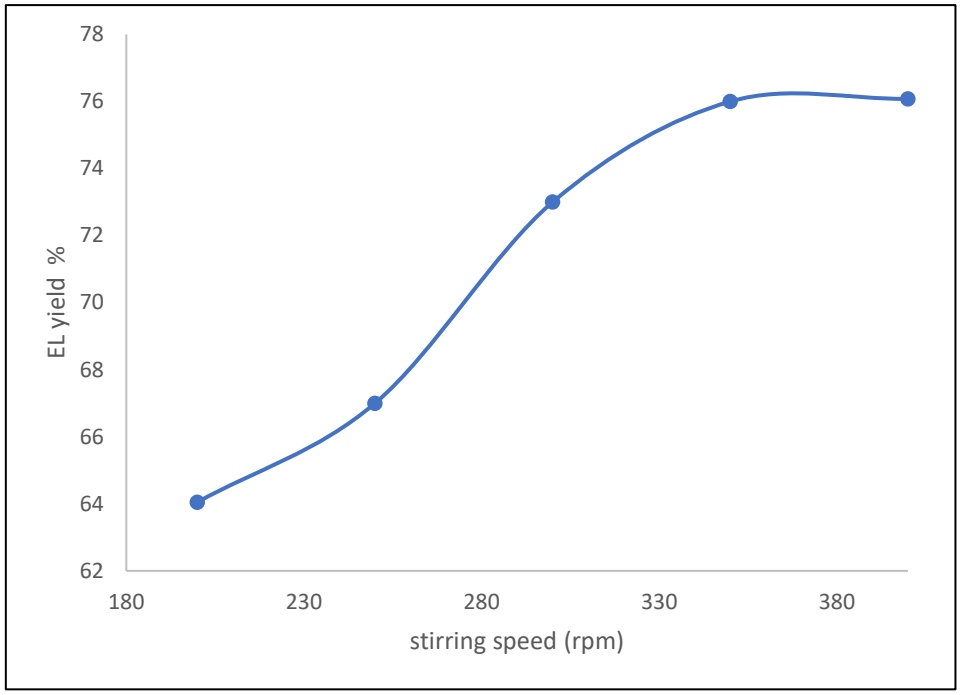

Figure 27. Effect of rotational speed on EL yield.

Reaction conditions: glucose 1g, temperature 140 ℃, catalyst loading 30 wt% and E/G 90.

Table 18: EL yield in different radiation systems under optimal conditions					
Radiation system	**Blank (no catalyst)**	**Conventional heating**	**UV only**	**IR only**	**Hybrid (UV+IR)**
EL yield	~4%	23.56%	25.88%	30.56%	76.08%

7.2.5. Reaction mechanism and pathway

Fig. 28 shows the reaction pathway and the various reaction intermediates involved in glucose conversion to ethyl levulinate. The very first step involves isomerization of glucose to fructose. This step is facilitated by a Lewis acid which in this case is provided by TiO_2. In the next step, fructose is converted to HMF through triple dehydration

process. This HMF, through successive rehydration and dehydration forms levulinic acid. In the next step LA reacts with ethanol to produce EL. All the latter steps are promoted by a Bronsted acid which in this case is provided by Amberlyst-36.

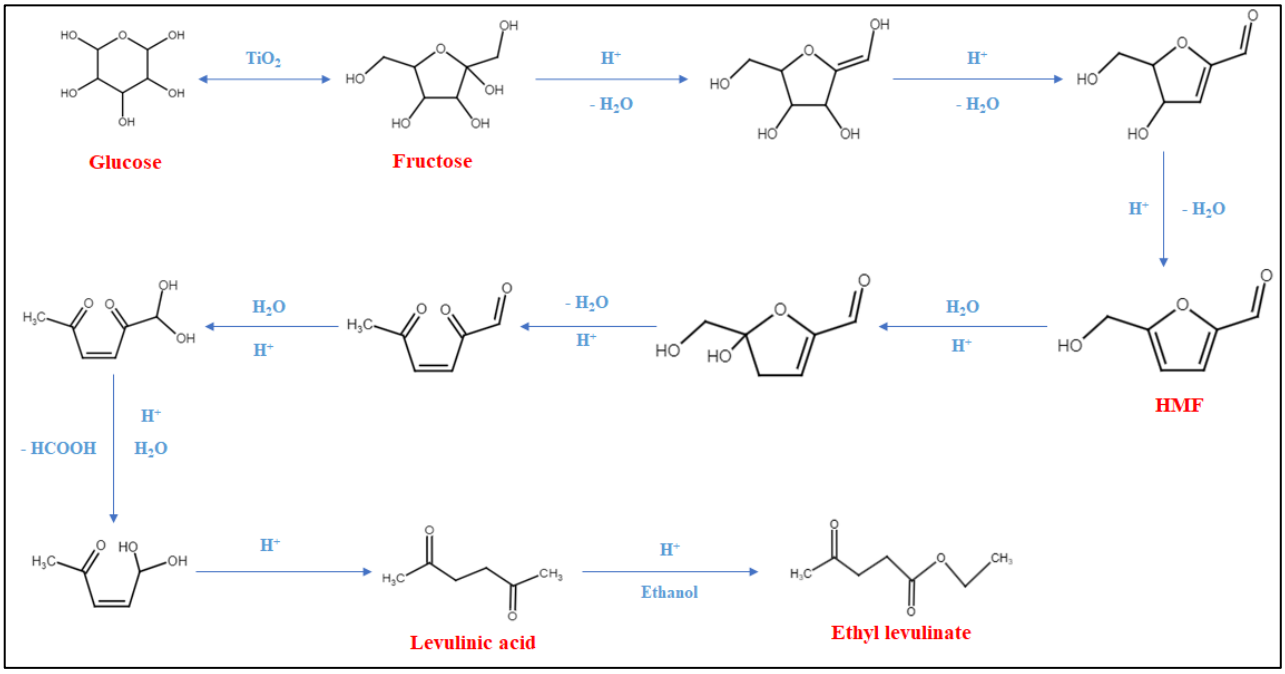

Figure 28. Reaction pathway for glucose conversion to EL.

As noticed in Fig 28, the reaction involves water molecules formed at the intermediate steps which also participates in the reaction and thus plays a pivotal role in the process. FIR radiation has been proven to excite water molecules by stretching and bending thus increasing particle collisions. Table 18 shows an EL yield of 30.56% when only FIR radiation has been used. While a 25.88% EL yield has been detected when only UV radiation was used. But when both the UV and FIR radiations were applied a whopping yield of 76.08% has been witnessed. This shows the synergistic effect of UV-FIR irradiation which is probably because UV radiation has excited the TiO_2 photocatalyst while IR has facilitated the steps involving water molecules and thus resulted in overall efficacy of the production process.

Table 19: Comparative study of EL production between current and previous publications

Feedstock	Catalyst	Reaction conditions (Temp, press, time, catalyst conc)	EL yield	Remarks	Ref
Glucose	H-USY + Amberlyst-15	96°C, 660 mins, 67 wt%	14%	• Higher time. • Higher catalyst loading. • Low yield.	52
Glucose	USY zeolite	180°C, 30 mins, 2.5 wt%	40%	• Higher temperature. • Low yield.	53
Glucose	H2SO4 + USY zeolite	180°C, 120 mins, 2.1 wt%	51.47%	• Higher temperature and time. • Use of H2SO4 makes	54

				product recovery difficult. • Low yield.	
Glucose	Hybrid zirconia zeolite catalyst	230°C, 360 mins, 30 wt%	21.9%	• Easy catalyst recovery for being magnetic. • Reaction temperature and time is very high. • Low yield.	55
Glucose	Sulfated ZrO_2	200°C, 180 mins, 2.5 wt%	30%	• Reaction temperature and time is very high. • Low yield.	56
Glucose	TiO_2+**Amberlyst-36**	**140 °C, 45 mins, 30 wt%**	**76.08%**	**Present study**	

7.2.6. Engine performance analysis

BSFC for all fuel blends increased with engine speed as shown in Fig. 29a. This is probably because increase in engine speed increases frictional losses and thus engine power did not increase much compared to fuel consumed. As for individual fuels, B7E3 showed lower BSFC than diesel and with further increase in EL quantity BSFC increased [91]. BTE of all the fuel types have been found to be lower than pure diesel and follows an analogous trend as compared to BSFC of the fuels as shown in Fig. 29b. The BP of all fuel blends were higher than pure diesel and exhibits a declining trend with an increase in EL content. which is in conformity with decreasing BTE. Fig. 29d shows the EGT of the fuels and it was noticed that all fuel blends showed lower EGT than pure diesel which implies higher combustion of the fuels [92].

7.2.7. Engine emissions

The engine exhaust emission quality for different fuel blends has been compared in Fig. 30. All the blended fuels showed lower hydrocarbon (HC) emissions than pure diesel (19 % reduction) and the hydrocarbon emission decreases with decrease in biodiesel content. This is probably because of better combustion of blended fuels owing to the availability of more oxygen in EL and biodiesel. The CO emission in Fig. 30b also shows similar trends (18.86 % reduction). The reason is more availability of oxygen and also lower C/H ratio in biodiesel and EL. The CO_2 in Fig. 30c emissions were higher for all fuel blends compared to diesel (59.09 % increase). This is due to more complete combustion and lower carbon content in biodiesel and EL. Also, with increase in EL content the CO_2 emission gets higher because EL has even lower carbon content than biodiesel. The NOx emission in Fig. 30d reveals that all fuel blends resulted higher

NOx formation than diesel (8.77 % increase). Also, NOx emission decreases with engine speed which can attributed to lower combustion time at higher speed [58].

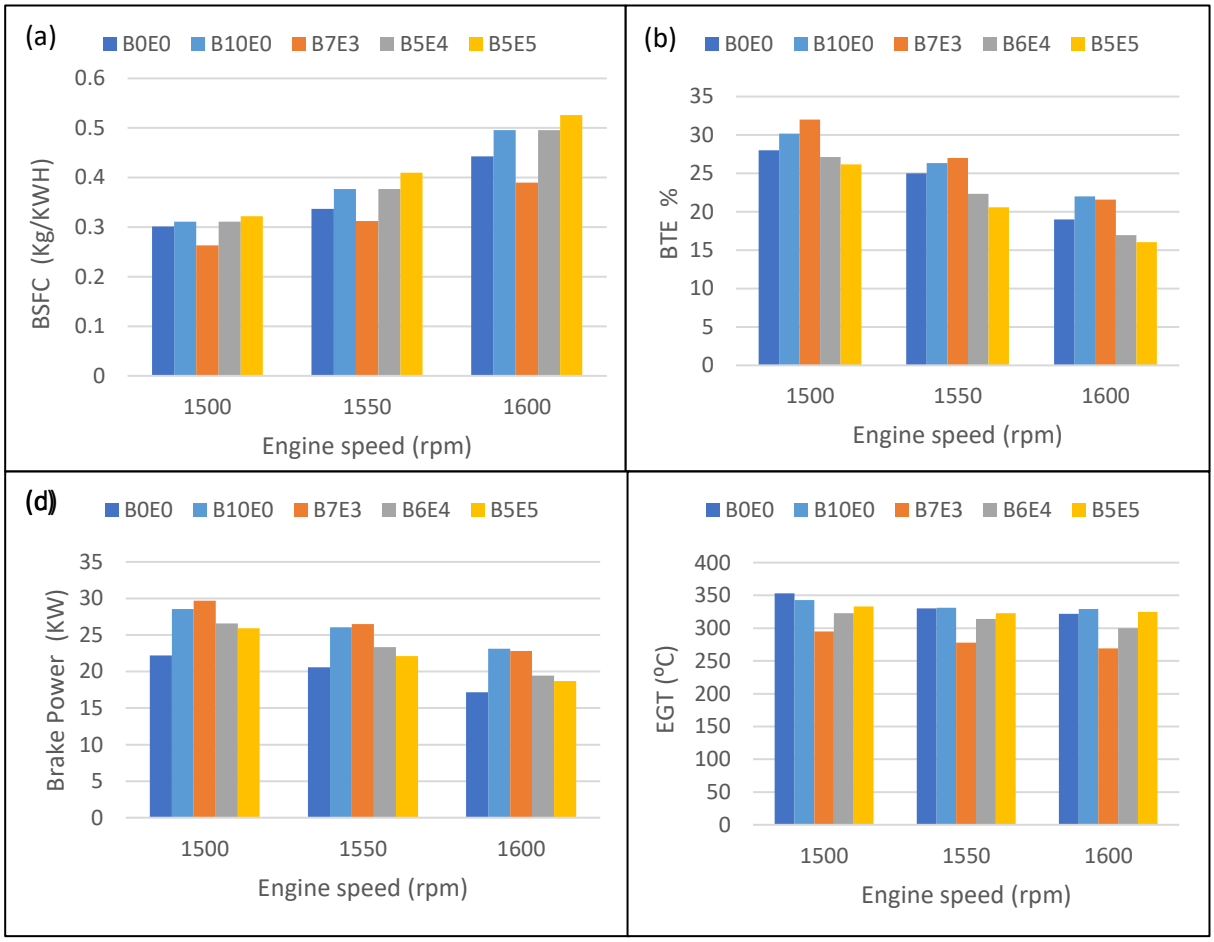

Figure 29. (a) BSFC, (b) BTE, (c) BP and (d) EGT for diesel and other fuel blends.

7.2.8. Life cycle impact assessment

The results of the environmental impact assessment utilizing ReCiPe Midpoint (H) v1.11 are depicted in Fig. 31. The LCA data for different process are tabulated in Table 20 and 21. The findings showed that the main impact indicators for both the systems comprised of global warming potential (GWP), fossil resource scarcity (FRS), terrestrial ecotoxicity (TE), human toxicity (HT) and terrestrial acidity (TA). The

photocatalytic conversion of glucose in ELHR resulted in less impacts in all categories in comparison to catalytic conversion in ELCH, as shown in Figure 8, which compares environmental effects of catalytic reaction in both types of reactors. The GWP was reduced by 48.86 %, FRS by 63.41% & TE by 84.21 % by using ELHR over ELCH.

The energy required to achieve an EL yield of 76.08% from glucose in ELHR (450 W, 45 mins) is 1.215 MJ, while to produce 58% EL in ELCH (500 W, 4.5 h), the energy required was 6.3 MJ. Hence the ELHR reactor is 5 times more energy efficient than ELCH system.

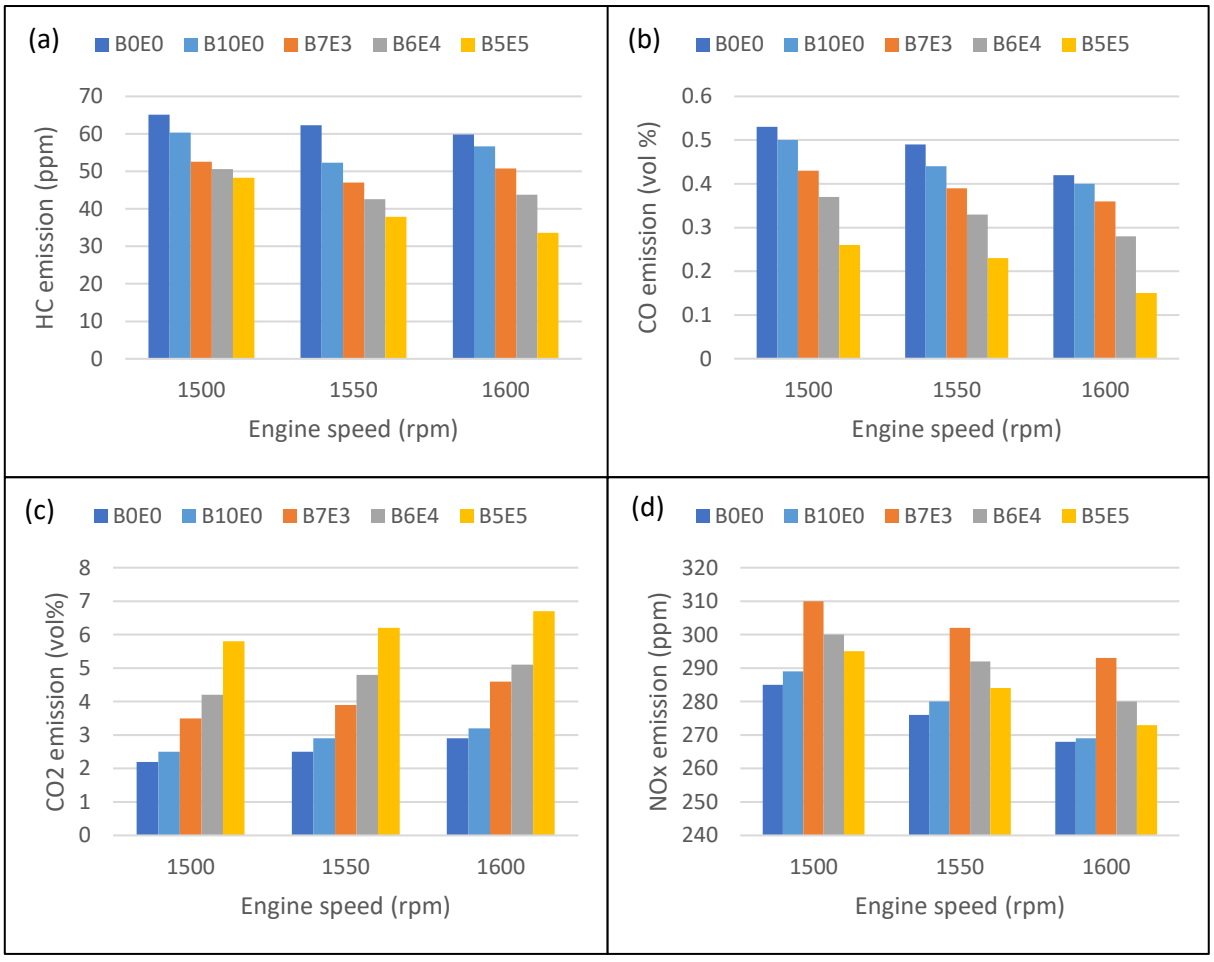

Figure 30. (a) HC, (b) CO, (c) CO_2 and (d) NOx emissions for diesel and other fuel blends.

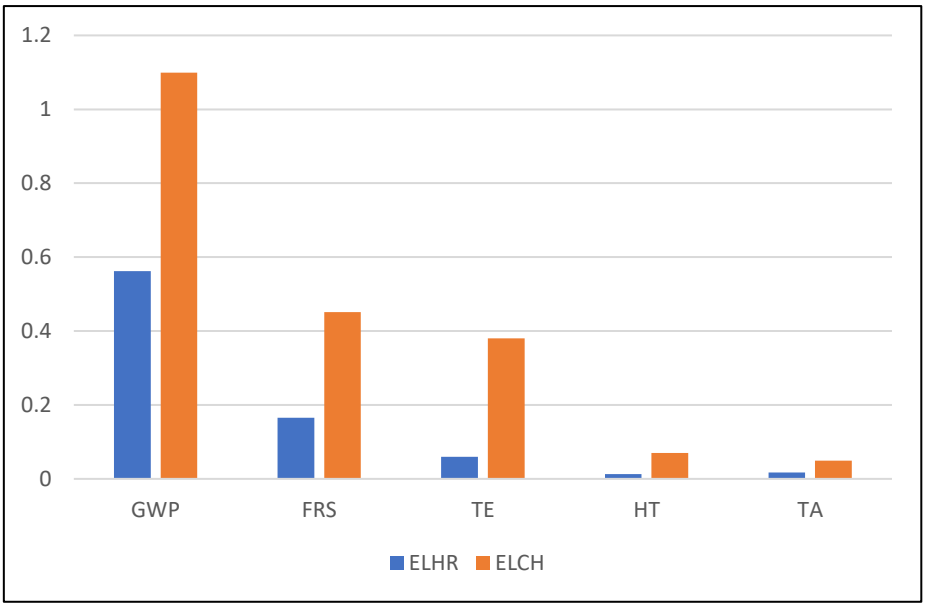

Figure 31. Comparative environmental impacts of ELHR and ELCH.

Table 20: LCI data to produce 1 kg EL in ELHR

Category	Flow	Value	Unit	Source
Energy Input	Electricity Consumption			
	For heating	1.215	MJ	Ecoinvent v3.9
	Stirring	0.028	MJ	Ecoinvent v3.9
	Vacuum evaporation	0.072	MJ	Ecoinvent v3.9
	Total	1.315	MJ	Ecoinvent v3.9
Material Input	Glucose	1.644	Kg	Ecoinvent v3.9
	Ethanol	37.829	kg	Ecoinvent v3.9
	TiO_2	0.164	Kg	Ecoinvent v3.9
	Amberlyst-36	0.329	Kg	Created
Emission to air	Waste heat	1.315	MJ	Ecoinvent v3.9
Material output	Ethanol	24.671	kg	Ecoinvent v3.9
Output	EL	1.00	kg	Created

Table 21: LCI data to produce 1 kg EL in ELCH

Category	Flow	Value	Unit	Source
Energy Input	Electricity Consumption			
	For heating	6.3	MJ	Ecoinvent v3.9
	Stirring	0.168	MJ	Ecoinvent v3.9
	Vacuum evaporation	0.1	MJ	Ecoinvent v3.9
	Total	6.568	MJ	Ecoinvent v3.9
Material Input	Glucose	2.174	Kg	Ecoinvent v3.9
	Ethanol	50	kg	Ecoinvent v3.9
	TiO_2	0.217	Kg	Ecoinvent v3.9
	Amberlyst-36	0.434	Kg	Created
Emission to air	Waste heat	6.568	KWh	Ecoinvent v3.9
Waste of Material	Ethanol	21.739	kg	Ecoinvent v3.9
Output	EL	1.00	kg	Created

Chapter 8

CONCLUSION

Conclusion

Waste fish scale and fly ash derived SiO2-Al2O3-HAp catalyst support impregnated with ZrO_2 active sites can sustainably produce levulinic acid from glucose at a low temperature of 115°C under UV-FIR irradiation. The prepared catalyst has a low band gap energy of 2.15 eV and high acidity of 1.52 mmol NH3/g and surface area of 62.872 m2/g which led to 76.6% levulinic acid yield at milder reaction conditions. Individual radiation effects as well as hybrid radiation effects have also been studied which reveals the efficacy of the synergistic effect of UV-IR hybrid irradiation. Furthermore, the catalyst showed good reusability after regeneration by calcination with no further decrease in LA yield up to 5th cycle suggesting absence of leaching of its active sites. LCA study revealed that photocatalytic conversion is more sustainable approach than conventional heating system with reduction in 59% global warming potential. Cost analysis revealed that cost of ZFH2 is INR 806.58 per kg. With these achievements in mind, it is our endeavor to prepare more efficient photocatalysts and study their performance in photo-continuous mode.

The present study also investigates the production of ethyl levulinate (EL) from glucose using various catalytic systems, employing a combination of Bronsted and Lewis acidic catalysts. A hybrid radiation approach is utilized to enhance the yield of EL. The optimal reaction conditions, including temperature, time, catalyst loading, and ethanol-to-glucose molar ratio, are determined to be 140°C, 45 minutes, 30wt%, and 90, respectively. The highest yield of EL, reaching 76.08%, is achieved using the Amberlyst-36 + TiO_2 catalytic system. The use of UV-IR hybrid irradiation is found to significantly increase the EL yield, potentially due to the excitation of TiO_2 by UV radiation and the promotion of particle collisions by FIR radiation. To assess engine performance and exhaust quality, the synthesized EL is blended with biodiesel and

diesel at various proportions. The blend B7E3 demonstrates the best performance, while it is observed that increasing the volume of EL in the fuel blend leads to a decrease in fuel quality in terms of engine performance and emission characteristics. The life cycle analysis (LCA) of EL production reveals that the hybrid radiation technique (ELHR) exhibits a 48.86% improvement in global warming potential (GWP) reduction compared to the conventional reactor (ELCH), with a five-fold decrease in energy consumption. Consequently, the hybrid radiation method proves to be an environmentally friendly and economically viable approach for EL production. These findings suggest that ethyl levulinate holds promise as a diesel fuel additive, and thus, it is crucial to develop a cost-effective production pathway at an industrial scale to address both global energy demands and air pollution issues.

Chapter 9

SCOPE OF WORK

Scope of work

Phase 1: Process Modification and Integration

- ✓ To conduct an extensive literature review to gather information on lignocellulosic biomass characteristics, its suitability as feedstock, and existing conversion processes.
- ✓ To create comprehensive model of the modified process using Aspen Plus software.
- ✓ To validate the model by comparing simulation results with available experimental data from the existing batch process.

Phase 2: Scale-up Analysis

- ✓ To conduct a feasibility study to assess the economic and technical viability of scaling up the process.
- ✓ To investigate the potential challenges and constraints in scaling up, and propose mitigation strategies.

Phase 3: Computational Fluid Dynamics (CFD) Analysis

- ✓ To develop a CFD model to study the fluid flow and mass transfer phenomena in photo-continuous reactor.
- ✓ To analyze reactor performance under different operating conditions and identify potential areas for improvement.

Phase 4: Exergy Analysis

- ✓ To perform an exergy analysis to evaluate the efficiency and sustainability of the modified process.
- ✓ To identify areas of energy loss and propose measures to enhance process efficiency.

Chapter 10

REFERENCES

References

1. Fells I. The problem. In: Dunderdale J, editor. Energy and the environment. UK: Royal Society of Chemistry, 1990.

2. IEA, Global share of total energy supply by source, 2019, IEA, Paris https://www.iea.org/data-and-statistics/charts/global-share-of-total-energy-supply-by-source-2019, IEA. Licence: CC BY 4.0.

3. Jimmy Nelson Appaturi, Jeyashelly Andas, Yik-Ken Ma, Bao Lee Phoon, Samaila Muazu Batagarawa, Fitri Khoerunnisa, M. Hazwan Hussin, Eng-Poh Ng. Recent advances in heterogeneous catalysts for the synthesis of alkyl levulinate biofuel additives from renewable levulinic acid: A comprehensive review. Fuel, 323, 2022, 124362.

4. Assary, R.S.; Redfern, P.C.; Hammond, J.R. Computational studies of the thermochemistry for conversion of glucose to levulinic acid. J. Phys. Chem. B 2010, 114, 9002–9009.

5. Yadav GD, Yadav AR. Synthesis of ethyl levulinate as fuel additives using heterogeneous solid superacidic catalysts: Efficacy and kinetic modeling. Chemical Engineering Journal. 2014 May 1;243:556-63.

6. Joshi H, Moser BR, Toler J, Smith WF, Walker T. Ethyl levulinate: A potential bio-based diluent for biodiesel which improves cold flow properties. Biomass and bioenergy. 2011 Jul 1;35(7):3262-6.

7. Lange JP, van de Graaf WD, Haan RJ. Conversion of furfuryl alcohol into ethyl levulinate using solid acid catalysts. ChemSusChem. 2009;2(5):437-441.

8. Lee A, Chaibakhsh N, Rahman MB, Basri M, Tejo BA. Optimized enzymatic synthesis of levulinate ester in solvent-free system. Industrial Crops and Products. 2010 Nov 1;32(3):246-51.

9. Zhu S, Chen C, Xue Y, Wu J, Wang J, Fan W. Graphene oxide: an efficient acid catalyst for alcoholysis and esterification reactions. ChemCatChem. 2014 Nov;6(11):3080-3.

10. Xu GZ, Chang C, Zhu WN, Li B, Ma XJ, Du FG. A comparative study on direct production of ethyl levulinate from glucose in ethanol media catalysed by different acid catalysts. Chemical Papers. 2013 Nov 1;67(11):1355-63.

11. Chang C, Xu G, Zhu W, Bai J, Fang S. One-pot production of a liquid biofuel candidate—Ethyl levulinate from glucose and furfural residues using a combination of extremely low sulfuric acid and zeolite USY. Fuel. 2015 Jan 15;140:365-70.

12. Liu R, Chen J, Huang X, Chen L, Ma L, Li X. Conversion of fructose into 5-hydroxymethylfurfural and alkyl levulinates catalyzed by sulfonic acid-functionalized carbon materials. Green chemistry. 2013;15(10):2895-903.

13. Kuo CH, Poyraz AS, Jin L, Meng Y, Pahalagedara L, Chen SY, Kriz DA, Guild C, Gudz A, Suib SL. Heterogeneous acidic TiO_2 nanoparticles for efficient conversion of biomass derived carbohydrates. Green Chemistry. 2014;16(2):785-91.

14. Yang Y, Hu C, Abu-Omar MM. Conversion of glucose into furans in the presence of AlCl3 in an ethanol–water solvent system. Bioresource technology. 2012 Jul 1;116:190-4..

15. Chakraborty R, Mukhopadhyay P, Kumar B. Energy Conversion and Management. 2016 Oct 15;126:32-41.

16. Pullen J, Saeed K. Factors affecting biodiesel engine performance and exhaust emissions–Part I. Energy. 2014 Aug 1;72:1-6.

17. Wang ZW, Lei TZ, Liu L, Zhu JL, He XF, Li ZF. Performance investigations of a diesel engine using ethyl levulinate diesel blends. BioResour 2012;7:5972-82.

18. Cañon C, Sanchez N, Cobo M. Sustainable production of ethyl levulinate by levulinic acid esterification obtained from Colombian rice straw. Journal of Cleaner Production. 2022 Dec 1;377:134276.

19. Szabolcs, A.; Molnár, M.; Dibó, G.; Mika, L.T. Microwave-assisted conversion of carbohydrates to levulinic acid: An essential step in biomass conversion. Green Chem. 2013, 15, 439–445.

20. Peng, L.; Lin, L.; Zhang, J.; Zhuang, J.; Zhang, B.; Gong, Y. Catalytic Conversion of Cellulose to Levulinic Acid by Metal Chlorides. Molecules 2010, 15, 5258–5272.

21. T.K. Tseng, et al., A review of photocatalysts prepared by sol-gel method for VOCs removal, Int. J. Mol. Sci. 11 (6) (2010) 2336.

22. U.I. Gaya, A.H. Abdullah, Heterogeneous photocatalytic degradation of organic contaminants over titanium dioxide: a review of fundamentals, progress and problems, J. Photochem. Photobiol. C 9 (1) (2008) 1–12.

23. F. Dong, H. Wang, Z. Wu, One-step “Green” synthetic approach for mesoporous doped titanium dioxide with efficient visible light photocatalytic activity, J. Phys. Chem. C 113 (38) (2009) 16717–16723.

24. H. Chen, C.E. Nanayakkara, V.H. Grassian, Titanium dioxide photocatalysis in atmospheric chemistry, Chem. Rev. 112 (11) (2012) 5919–5948.

25. K. Nakata, A. Fujishima, TiO_2 photocatalysis: design and applications, J. Photochem. Photobiol. C 13 (3) (2012) 169–189.

26. Szabolcs, A.; Molnár, M.; Dibó, G.; Mika, L.T. Microwave-assisted conversion of carbohydrates to levulinic acid: An essential step in biomass conversion. Green Chem. 2013, 15, 439–445.

27. Van Zandvoort I, Wang Y, Rasrendra CB, van Eck ER, Bruijnincx PC, Heeres HJ, Weckhuysen BM. Formation, molecular structure, and morphology of humins in biomass conversion: influence of feedstock and processing conditions. ChemSusChem. 2013 Sep;6(9):1745-58.

28. Rackemann, D.W.; Bartley, J.P.; Doherty, W.O.S. Methanesulfonic acid-catalyzed conversion of glucose and xylose mixtures to levulinic acid and furfural. Ind. Crops Prod. 2014, 52, 46–57.

29. Choudhary, V.; Mushrif, S.H.; Ho, C.; Anderko, A.; Nikolakis, V.; Marinkovic, N.S.; Frenkel, A.I.; Sandler, S.I.; Vlachos, D.G. Insights into the Interplay of Lewis and Brønsted Acid Catalysts in Glucose and Fructose Conversion to 5-(Hydroxymethyl)furfural and Levulinic Acid in Aqueous Media. J. Am. Chem. Soc. 2013, 135, 3997–4006.

30. Peng, L.; Lin, L.; Zhang, J.; Zhuang, J.; Zhang, B.; Gong, Y. Catalytic Conversion of Cellulose to Levulinic Acid by Metal Chlorides. Molecules 2010, 15, 5258–5272.

31. Shen Y, Xu Y, Sun J, Wang B, Xu F, Sun R. Efficient conversion of monosaccharides into 5-hydroxymethylfurfural and levulinic acid in InCl 3 –H 2 O medium. Catal Commun 2014;50(14):17–20.

32. Fu, J., Yang, F., Mo, J., Zhuang, J., and Lu, X. (2015). "Catalytic decomposition of glucose to levulinic acid by synergy of organic Lewis acid and Brønsted acid in water," BioRes. 10(1), 1346-1356.

33. Zuo, Y.; Zhang, Y.; Fu, Y. Catalytic Conversion of Cellulose into Levulinic Acid by a Sulfonated Chloromethyl Polystyrene Solid Acid Catalyst. ChemCatChem 2014, 6, 753–757.

34. Son, P.A.; Nishimura, S.; Kohki Ebitani, K. Synthesis of levulinic acid from fructose using Amberlyst-15 as a solid acid catalyst. React. Kinet. Mech. Catal. 2012, 106, 185–192.

35. Zeng, W.; Cheng, D.G.; Chen, F.; Zhan, X. Catalytic Conversion of Glucose on Al–Zr Mixed Oxides in Hot Compressed Water. Catal. Lett. 2009, 133, 221–226.

36. Ya'aini, N.; Saidina Amin, N.A.; Endud, S. Characterization and performance of hybrid catalysts for levulinic acid production from glucose. Microporous Mesoporous Mater. 2013, 171, 14–23.

37. Ramli, N.A.S.; Saidina Amin, N.A. Kinetic study of glucose conversion to levulinic acid over Fe/HY zeolite catalyst. Chem. Eng. J. 2016, 283, 150–159.

38. Upare, P.P.; Yoon, J.W.; Kim, M.Y.; Kang, H.Y.; Hwang, D.W.; Hwang, Y.K.; Kung, H.H.; Chang, J.S. Chemical conversion of biomass-derived hexose sugars to levulinic acid over sulfonic acid-functionalized graphene oxide catalysts. Green Chem. 2013, 15, 2935–2943.

39. Kumar VB, Pulidindi IN, Mishra RK, Gedanken A. Development of Ga salt of molybdophosphoric acid for biomass conversion to levulinic acid. Energy Fuels 2016;30(12):10583–91.

40. Zeng W, Cheng DG, Zhang H. Dehydration of glucose to levulinic acid over MFI-type zeolite in subcritical water at moderate conditions. React Kinet Mech Catal 2010;100(2):377–84.

41. Wang Y, Nie X. Preparation of magnetic solid acid catalyst S 2 O 8 2−/ZrO 2–TiO 2–Fe 3 O 4 and its application to synthesis of levulinic acid. J. Cent. South Univ. Sci. Technol. 2016;1:26-32.

42. Joshi SS, Zodge AD, Pandare KV, Kulkarni BD. Efficient conversion of cellulose to levulinic acid by hydrothermal treatment using zirconium dioxide as a recyclable solid acid catalyst. Ind Eng Chem Res 2014;53(49):18796–805.

43. Ding D, Wang J, Xi J, Liu X, Lu G, Wang Y. High-yield production of levulinic acid from cellulose and its upgrading to γ-valerolactone. Green Chem 2014;16(8):685–93.

44. Liu Y, Li H, He J, Zhao W, Yang T, Yang S. Catalytic conversion of carbohydrates to levulinic acid with mesoporous niobium-containing oxides. Catal Commun 2017;93:20–4.

45. I. Abdouli, F. Dappozze, M. Eternot, N. Essayem, C. Guillard. Hydrothermal process assisted by photocatalysis: Towards a novel hybrid mechanism driven glucose valorization to levulinic acid, ethylene and hydrogen. Applied Catalysis B: Environmental 305 (2022) 121051.

46. Qu Y, Zhao Y, Xiong S, Wang C, Wang S, Zhu L, Ma L. Conversion of glucose into 5-hydroxymethylfurfural and levulinic acid catalysed by SO_4^{2-}/ ZrO_2 in a biphasic solvent system. Energy & Fuels. 2020 Aug 3;34(9):11041-9.

47. Jow J, Rorrer GL, Hawley MC, Lamport DT. Dehydration of D-fructose to levulinic acid over LZY zeolite Catalyst. Biomass 1987;14:185–94.

48. Chen, H.; Yu, B.; Jin, S. Production of levulinic acid from steam exploded rice straw via solid superacid, $S_2O_8^{2-}$/ ZrO_2–SiO_2–Sm_2O_3. Bioresour. Technol. 2011, 102, 3568–3570.

49. Shen F, Jr RL S, Li L, Yan L, Qi X. Eco-friendly method for efficient conversion of cellulose into levulinic acid in pure water with cellulase-mimetic solid acid catalyst. ACS Sustain Chem Eng 2017;5(3):2421–7.

50. Liu W, Hou Y, Wu W, Liu Z, Liu Q, Tian S, Marsh KN. Efficient conversion of cellulose to glucose, levulinic acid, and other products in hot water using SO_2 as a recoverable catalyst. Ind Eng Chem Res 2012;51(47):15503–8.

51. Pyo SH, Glaser SJ, Rehnberg N, Hatti-Kaul R. Clean production of levulinic acid from fructose and glucose in salt water by heterogeneous catalytic dehydration. ACS omega. 2020 Jun 11;5(24):14275-82.

52. Li H, Saravanamurugan S, Yang S, Riisager A. Direct transformation of carbohydrates to the biofuel 5-ethoxymethylfurfural by solid acid catalysts. Green Chemistry. 2016;18(3):726-34.

53. Xu GZ, Chang C, Zhu WN, Li B, Ma XJ, Du FG. A comparative study on direct production of ethyl levulinate from glucose in ethanol media catalysed by different acid catalysts. Chemical Papers. 2013 Nov 1;67(11):1355-63.

54. Chang C, Xu G, Zhu W, Bai J, Fang S. One-pot production of a liquid biofuel candidate—Ethyl levulinate from glucose and furfural residues using a combination of extremely low sulfuric acid and zeolite USY. Fuel. 2015 Jan 15;140:365-70.

55. Li H, Fang Z, Yang S. Direct conversion of sugars and ethyl levulinate into γ-valerolactone with superparamagnetic acid–base bifunctional ZrFeO x nanocatalysts. ACS Sustainable Chemistry & Engineering. 2016 Jan 4;4(1):236-46.

56. Peng L, Lin L, Zhang J, Shi J, Liu S. Solid acid catalyzed glucose conversion to ethyl levulinate. Applied Catalysis A: General. 2011 Apr 30;397(1-2):259-65.

57. Mukhopadhyay P, Chakraborty R. Infrared radiation promoted preparation of cost-effective lamb bone supported cobalt catalyst: Efficacy in semi-batch monoolein synthesis. Catalysis Communications. 2017 May 5;94:73-6.

58. Lei T, Wang Z, Chang X, Lin L, Yan X, Sun Y, Shi X, He X, Zhu J. Performance and emission characteristics of a diesel engine running on optimized ethyl levulinate–biodiesel–diesel blends. Energy. 2016 Jan 15;95:29-40.

59. Betke U, Scheunemann M, Scheffler M. Refitting of zirconia toughening into open-cellular alumina foams by infiltration with zirconyl nitrate. Materials. 2019 Jun 12;12(12):1886.

60. R.N. Panda, M.F. Hsieh, R.J. Chung, T.S. Chin. FTIR, XRD, SEM and solid-state NMR investigations of carbonate-containing hydroxyapatite nano-particles synthesized by hydroxide-gel technique. Journal of Physics and Chemistry of Solids 64 (2003) 193–199.

61. N. Singh, R. Chakraborty, R. K. Gupta. Mutton bone derived hydroxyapatite supported TiO_2 nanoparticles for sustainable photocatalytic applications. Journal of Environmental Chemical Engineering 6 (2018) 459–467.

62. J S Earl, D J Wood and S J Milne. Hydrothermal synthesis of hydroxyapatite. Journal of Physics: Conference Series 26 (2006) 268–271.

63. K. Gnanamoorthi, M. Balakrishnan, R. Mariappan, E. Ranjith Kumar. Effect of Ce doping on microstructural, morphological and optical properties of ZrO_2 nanoparticles. Materials Science in Semiconductor Processing 30 (2015) 518–526.

64. R. Naghizadeh, F. Golestani-fard, H.R. Rezaie. Stability and phase evolution of mullite in reducing atmosphere. Materials characterization 62 (2011) 540–544.

65. F. Bollino, E. Armenia, E. Tranquillo. Zirconia/Hydroxyapatite Composites Synthesized Via Sol-Gel: Influence of Hydroxyapatite Content and Heating on Their Biological Properties. Materials 2017, 10, 757.

66. R. Chakraborty, P. Mukhopadhyay, B. Kumar. Optimal biodiesel-additive synthesis under infrared excitation using pork bone supported-Sb catalyst: Engine performance and emission analyses Energy Conversion and Management 126 (2016) 32–41.

67. Alzeer MI, MacKenzie KJ. Synthesis and catalytic properties of new sustainable aluminosilicate heterogeneous catalysts derived from fly ash. ACS Sustainable Chemistry & Engineering. 2018 Mar 13;6(4):5273-82.

68. NIST X-ray Photoelectron Spectroscopy Database, Version 4.1 (National Institute of Standards and Technology, Gaithersburg, 2012); http://srdata.nist.gov/xps/.

69. S. Roy Choudhury, R. Chakraborty. Sustainable Total Reducing Sugar Production by Waste Printed Power Board Derived Zn–Zr Photocatalyst. Waste Biomass Valor (2022).

70. M. Paukov, I. Tkach, F. Huber, T. Gouder, M. Cieslar, D. Drozdenko, P. Minarik, L. Havela. U-Zr alloy: XPS and TEM study of surface passivation. Applied Surface Science 441 (2018) 113–119.

71. M. A. Stranick, M. J. Root. Influence of strontium on monofluorophosphate uptake by hydroxyapatite XPS characterization of the hydroxyapatite surface. Colloids and Surfaces, 55 (1991) 137-147.

72. B. Demri, D. Muster. XPS study of some calcium compounds. Journal of Materials Processing Technology 55 (1995) 311-314.

73. B. M. Reddy, P. M. Sreekanth, Y. Yamada, Q. Xu, T. Kobayashi. Surface characterization of sulfate, molybdate and tungstate promoted TiO_2- ZrO_2 solid acid catalysts by XPS and other techniques. Applied Catalysis A: General 228 (2002) 269–278.

74. A. Z. Johannes, R. K. Pingak, M. Bukit. Tauc Plot Software: Calculating energy gap values of organic materials based on Ultraviolet-Visible absorbance spectrum. IOP Conf. Ser.: Mater. Sci. Eng. 823 012030.

75. V.R. Sivaperumal, R. Mani, V. Polisetti, K. Aruchamy, T. Oh. Synthesis of Hydroxyapatite (HAp)-Zirconia Nanocomposite Powder and Evaluation of Its Biocompatibility: An In Vitro Study. Appl. Sci. 2022, 12, 11056.

76. R. Pazhani, H. Padma Kumar, Angeo Varghese, A. Moses Ezhil Raj, Sam Solomon, J.K. Thomas. Synthesis, vacuum sintering and dielectric characterization of zirconia (t-ZrO 2) nanopowder. Journal of Alloys and Compounds 509 (2011) 6819–6823.

77. Chatterjee A, Hu X, Lam FL. Catalytic activity of an economically sustainable fly-ash-metal-organic-framework composite towards biomass valorization. Catalysis Today. 2018 Sep 15;314:137-46.

78. P. Mukhopadhyay, R. Chakraborty. Heterogeneous esterification kinetics of isopropyl oleate synthesis under non-ionizing excitation using nano-anatase imbued mesoporous catalyst. Chemical Engineering Communications (2019) 206:7, 871-887.

79. Haag WO, Lago RM, Weisz PB. The active site of acidic aluminosilicate catalysts. Nature. 1984 Jun 14;309(5969):589-91.

80. Mukhopadhyay P, Chakraborty R. Energy-Efficient 2-Ethylhexyl Acetate Synthesis with a Nano-Sn-Hydroxyapatite Photocatalyst. Chemical Engineering & Technology. 2020 Mar;43(3):531-9.

81. K. Anand, K. Kaviyarasu, Sudhakar Muniyasamy, Selvaraj Mohana Roopan, R. M. Gengan, A. A. Chuturgoon. Bio-Synthesis of Silver Nanoparticles Using Agroforestry Residue and Their Catalytic Degradation for Sustainable Waste Management. J Clust Sci (2017) 28:2279–2291.

82. Rackemann DW, Doherty WO. The conversion of lignocellulosics to levulinic acid. Biofuels, Bioproducts and Biorefining. 2011 Mar;5(2):198-214.

83. Kumar VB, Pulidindi IN, Mishra RK, Gedanken A. Development of Ga salt of molybdophosphoric acid for biomass conversion to levulinic acid. Energy Fuels 2016;30(12):10583–91.

84. Ya'Aini N, Amin NAS, Endud S. Characterization and performance of hybrid catalysts for levulinic acid production from glucose. Microporous Mesoporous Mater 2013;171(171):14–23.

85. Á. Szabolcs, M. Molnár, G. Dibó, L. T. Mika. Microwave-assisted conversion of carbohydrates to levulinic acid: an essential step in biomass conversion. Green Chem., 2013, 15, 439-445.

86. I. Abdouli, F. Dappozze, M. Eternot, N. Essayem, C. Guillard. Hydrothermal process assisted by photocatalysis: Towards a novel hybrid mechanism driven glucose valorization to levulinic acid, ethylene and hydrogen. Applied Catalysis B: Environmental 305 (2022) 121051.

87. Son, P.A., Nishimura, S. & Ebitani, K. Preparation of zirconium carbonate as water-tolerant solid base catalyst for glucose isomerization and one-pot synthesis of levulinic acid with solid acid catalyst. Reac Kinet Mech Cat 111, 183–197 (2014).

88. Qu Y, Zhao Y, Xiong S, Wang C, Wang S, Zhu L, Ma L. Conversion of glucose into 5-hydroxymethylfurfural and levulinic acid catalysed by SO_4^{2-}/ ZrO_2 in a biphasic solvent system. Energy & Fuels. 2020 Aug 3;34(9):11041-9.

89. Zeng, W., Cheng, Dg., Zhang, H. et al. Dehydration of glucose to levulinic acid over MFI-type zeolite in subcritical water at moderate conditions. Reac Kinet Mech Cat 100, 377–384 (2010).

90. Karan P, Chakraborty R. Intensification of autocatalytic methyl oleate synthesis in continuous flow rotating recycle reactor under hybrid radiation: Process optimization and Scale-up. Chemical Engineering Journal. 2023 Jan 1;455:140032.

91. Wang ZW, Lei TZ, Liu L, Zhu JL, He XF, Li ZF. Performance investigations of a diesel engine using ethyl levulinate-diesel blends. BioResources. 2012 Nov 1;7(4).

92. Mukhopadhyay P, Chakraborty R. LCA of sustainable biodiesel production from fried Borassus flabellifer oil in energy-proficient reactors: Impact assessment of multi fuel-additives on pour point, NOx and engine performance. Sustainable Energy Technologies and Assessments. 2021 Apr 1;44:100994.

Appendix-I

Appendix-II